



Contents lists available at SciVerse ScienceDirect

Gondwana Research

journal homepage: www.elsevier.com/locate/gr

U–Pb zircon ages for Yarlung Tsangpo suture zone ophiolites, southwestern Tibet and their tectonic implications

Gavin Heung Ngai Chan ^{a,e}, Jonathan C. Aitchison ^{b,e,*}, Quentin G. Crowley ^{c,d}, Matthew S.A. Horstwood ^c, Michael P. Searle ^a, Randall R. Parrish ^c, Jacky Sik-Lap Chan ^e

^a Department of Earth Sciences, Oxford University, Parks Road, Oxford, OX1 3PR, UK

^b School of Geosciences, The University of Sydney, Sydney, NSW 2006, Australia

^c NIGL, British Geological Survey, Keyworth, Nottingham, NG12 5GG, UK

^d Department of Geology, School of Natural Sciences, Trinity College, Dublin 2, Ireland

^e Department of Earth Sciences, The University of Hong Kong, Pokfulam Road, Hong Kong, China

ARTICLE INFO

Article history:

Received 9 January 2013

Received in revised form 21 May 2013

Accepted 14 June 2013

Available online xxx

Keywords:

Ophiolites

Tethys

U/Pb ages

India–Asia collision

Tibet

ABSTRACT

Ophiolite complexes preserved along the Yarlung Tsangpo suture zone (YTSZ) and obducted onto the northern continental margin of India in southern Tibet represent the remnants of the once extensive Permian–Mesozoic Neo-Tethyan Ocean that separated India from Asia. Complete ophiolite successions are preserved near Xigaze, whereas the rest of the belt is essentially represented by mantle rocks with subordinate disrupted lower crustal rocks. U–Pb zircon LA-MC-ICP-MS geochronology on two gabbro samples from the Luobusa ophiolite yielded concordant data with mean $^{206}\text{Pb}/^{238}\text{U}$ ages of 149.9 ± 1.4 (2σ) Ma and 150.0 ± 5.0 Ma. These ages are in contrast to a younger age of 131.8 ± 1.0 Ma obtained from a pegmatitic gabbro in Xigaze. Five U–Pb zircon TIMS ages from gabbroic samples in the western portion of the ophiolite belt reveal that the Dangxiong ophiolite formed between 126.7 ± 0.4 Ma and 123.4 ± 0.8 Ma. Zircons from the Jungbwa ophiolite have similar ages of 123.4 ± 0.8 Ma and 123.9 ± 0.9 Ma. A single zircon analysed from a gabbro in Kiogar has an age of 159.7 ± 0.5 Ma. Geochronological data reported here show YTSZ ophiolites formed in association with intra-oceanic subduction zone systems and are related to a significant tectonic episode within the Tethyan Ocean during Late Jurassic to Early to mid Cretaceous times.

© 2013 International Association for Gondwana Research. Published by Elsevier B.V. All rights reserved.

1. Introduction

The India–Asia collision is marked by the Yarlung Tsangpo suture zone (YTSZ) in southern Tibet and beyond into northern India along the correlative Indus suture. For at least 2500 km this suture forms the boundary between the Tethyan Himalaya of the Indian plate to the south and the collage of plates that make up Asia to the north. Ophiolite complexes, preserved both along the suture and obducted onto the northern margin of India, provide our only evidence of the age and composition of the once extensive Neo-Tethyan Ocean that separated India from the Lhasa Block on southern margin of Eurasia. Early interpretations indicated that the YTSZ ophiolites were formed in a mid-ocean ridge (MOR) environment and consumed along a single zone of convergence along the southern margin of Eurasia (Nicolas et al., 1981; Allegre et al., 1984; Girardeau et al., 1985b; Wang et al., 1987). In contrast, recent work (summarized in Hébert et al., 2012) has shown that most ophiolites possess supra-subduction zone (SSZ) geochemical signatures, except for portions of the Luobusa ophiolite in

SE Tibet, parts of the Jungbwa massif in SW Tibet and the lower part of the Spontang ophiolite in northern India (Corfield et al., 2001), where evidence for MOR-type magmatism is preserved. Moreover, rocks associated with at least phases of two intra-oceanic island arc development have been recognized along the suture (Aitchison et al., 2000; Corfield et al., 2001; Malpas et al., 2003; Miller et al., 2003; Mahéo et al., 2004; Hébert et al., 2012). Most Himalayan–Tibetan ophiolites are thought to have been emplaced onto the northern passive margin of the Indian plate during Late Cretaceous–Paleocene times (Searle, 1983; Allegre et al., 1984; Searle, 1986; Searle et al., 1997; Aitchison et al., 2000; Davis et al., 2002; Malpas et al., 2003; Aitchison and Davis, 2004; Ding et al., 2005; Aitchison et al., 2007a; Guilmette et al., 2009, 2012; Hébert et al., 2012).

One of the keys to advancing the understanding YTSZ zone ophiolites is to constrain the time at which magmatic rocks crystallised and during formation of the ophiolites. The published age data from these ophiolites are (summarized in Hébert et al., 2012) and shown in Fig. 1. Biostratigraphic dating suggests that the Xigaze ophiolite was formed in the Early Cretaceous (Ziabrev et al., 2003), which is in accordance with the U–Pb zircon ages (Göpel et al., 1984; Malpas et al., 2003; Wang et al., 2006). Other U–Pb zircon ages ranging from Jurassic to Late Cretaceous have been published for published from the Zedong, Dangxiong,

* Corresponding author at: School of Geosciences, The University of Sydney, Sydney, NSW 2006, Australia. Tel.: +61 93513244.

E-mail address: jonathan.aitchison@sydney.edu.au (J.C. Aitchison).

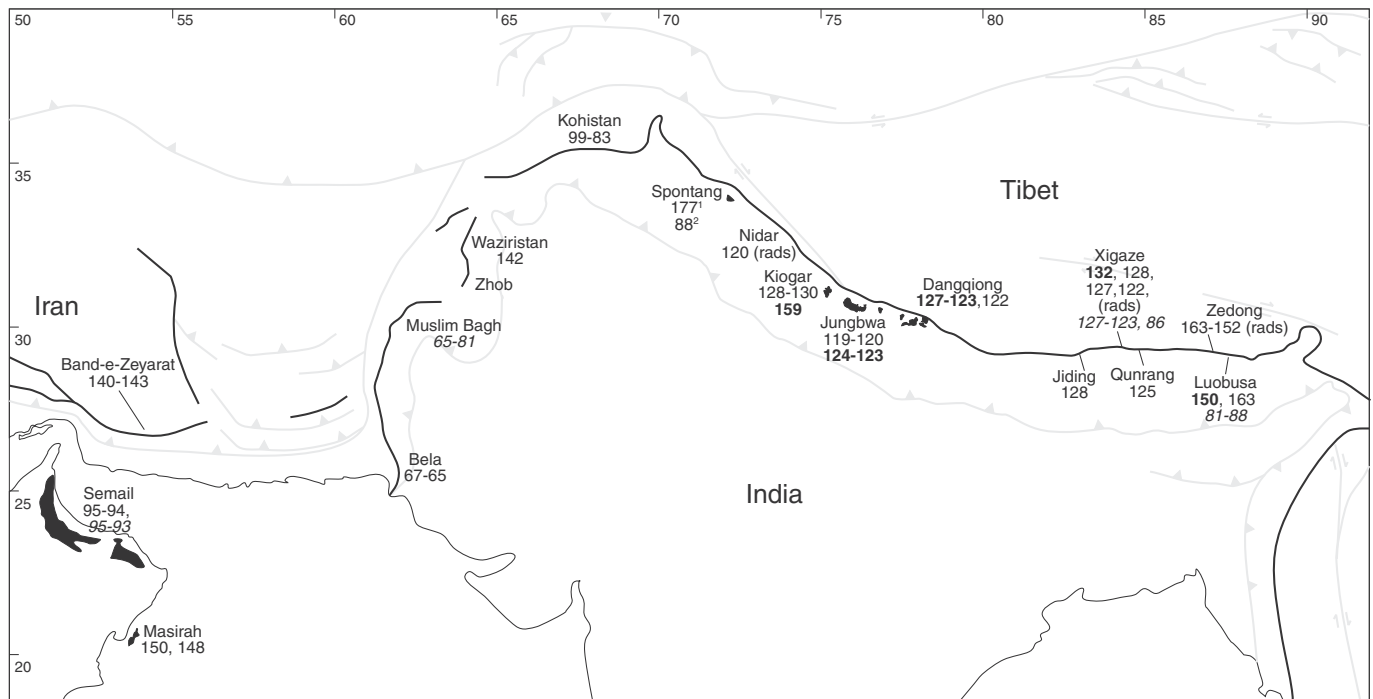


Fig. 1. Ophiolites and ophiolitic suture zones (black) and their ages. All dates are radiometric U–Pb zircon or ^{40}Ar – ^{39}Ar amphibole ages. Igneous crystallization ages are shown in normal font (bold font are results of current study); metamorphic sole ages are italicized. Locations from which radiolarian faunas have been extracted from intercalated or overlying cherts are indicated by (rads). Sources of data: Semail (Hacker, 1994; Hacker and Gnos, 1997; Warren et al., 2003), Band-e-Zeyarat (Ghazi et al., 2004), Bela (Ahmed, 1993), Muslim Bagh (Mahmood et al., 1995; Kakar et al., 2012), Waziristan (Khan et al., 2007), Kohistan (Schaltegger et al., 2002). Spontang¹–MORB-type sequence, ²–island arc sequence (Pedersen et al., 2001), Nidar (Zyabrev et al., 2008), KioGAR (Xiong et al., 2011), Jungbwa (Li et al., 2008; Xia et al., 2011), Dangxiong (Wei et al., 2006), Jiding (Wang et al., 2006), Xigaze (Malpas et al., 2003; Ziabrev et al., 2003; Wang et al., 2006; Guilmette et al., 2009; Li et al., 2009), Zedong (McDermid et al., 2002) and Luobusa (Malpas et al., 2003; Zhong et al., 2006b).

Spontang and Muslim Bagh ophiolites (Pedersen et al., 2001; McDermid et al., 2002; Wei et al., 2006; Kakar et al., 2012). Ages determined using other isotopic systems such as Sm–Nd have large errors and do not constrain formation of the ophiolite crustal sequence. High-grade metamorphic rocks have been commonly found within the sub-ophiolitic melanges (Guilmette et al., 2007, 2009, 2012). These metamorphic sole rocks are traditionally interpreted as derived from metamorphic soles formed beneath the ophiolites during their initial intra-oceanic displacement (e.g. Williams and Smythe, 1973; Malpas, 1979; Searle and Malpas, 1982; Wakabayashi and Dilek, 2000; Searle and Cox, 2002). Although their ages potentially provide important constraints on obduction processes some recent work suggests that such metamorphic rocks may be associated with ophiolite generation rather than emplacement (Dewey and Casey, 2011). In this paper we present new U–Pb zircon ages for five different massifs of the YTSZ ophiolites from southeastern to southwestern Tibet (Luobusa, Xigaze, Dangxiong, Jungbwa and KioGAR). We use these data to determine the timing of ophiolite genesis and elucidate how these ages might be related to the inferred timing of intra-oceanic displacement, emplacement onto Indian continental margin and ultimate incorporation into the Himalayan orogenic belt.

2. Background

2.1. Regional geology

The southern margin of the Tibetan plateau is characterized by a number of east–west trending terranes. From the north to the south, it is marked by the Lhasa terrane, which incorporates the Jurassic to Eocene Gangdese batholith and associated Linzizong extrusives. The Gangdese granites have U–Pb zircon ages as old as 205 Ma and as young as 34 Ma (Ji et al., 2012) with the majority of rocks dated thus far between 65 and 41 Ma (Ji et al., 2009). The calc-alkaline Linzizong

volcanics (andesites, dacites, rhyolites) are the extrusive component to the Gangdese granites and have $^{40}\text{Ar}/^{39}\text{Ar}$ ages ranging from Cretaceous to Eocene with the majority of data suggesting the most extensive component erupted around 50 Ma (Lee et al., 2009). South of the granitic Gangdese batholith lie a series of Mid-Late Cretaceous forearc volcanoclastic turbidites (Xigaze terrane) that were derived from a source region to the north (Dürr, 1996; Aitchison et al., 2011; Wang et al., 2012). The suture zone between India and Eurasia itself consists of a series of dismembered ophiolites and associated rocks of the Cretaceous Dazhuqu terrane (Aitchison et al., 2000). Other structural domains include examples of a series of Mid-Jurassic intra-oceanic arc rocks (Zedong terrane) and a Cretaceous subduction-related accretionary complex (Bainang terrane), occurring elsewhere along the suture zone (Aitchison et al., 2000 and references therein).

2.2. Luobusa massif and associated Zedong terrane ophiolitic rocks

The Luobusa massif is c. 1 km thick and extends for c. 40 km in an east–west direction, occurring to the immediate north of Luobusa Village in southeast Tibet (Fig. 2a). Although elsewhere ophiolitic massifs are generally thrust southward onto the northern margin of India as Luobusa post collisional back-thrusting along the Great Counter thrust (Gansser, 1964) has resulted in northward emplacement of the massif above an ophiolitic melange, which in turn is thrust over Lower Miocene Gangrinboche conglomerates (Aitchison et al., 2002b, 2009). To the south, the ophiolite is overthrust by rocks of Indian affinity (Zhou et al., 1996; Yamamoto et al., 2007). The bulk of the ophiolite is essentially represented by a mantle sequence, which comprises harzburgite, dunite and chromitite. The chromitites host a variety of rare ultrahigh-pressure minerals such as diamond, moissanite, native metal and PGE alloys (Bai et al., 1993, 2000; Robinson et al., 2004). Elsewhere, these mantle rocks are further cut by diabase and gabbro dykes. The details of petrographical and geochemical relationships of the Luobusa ophiolite have been

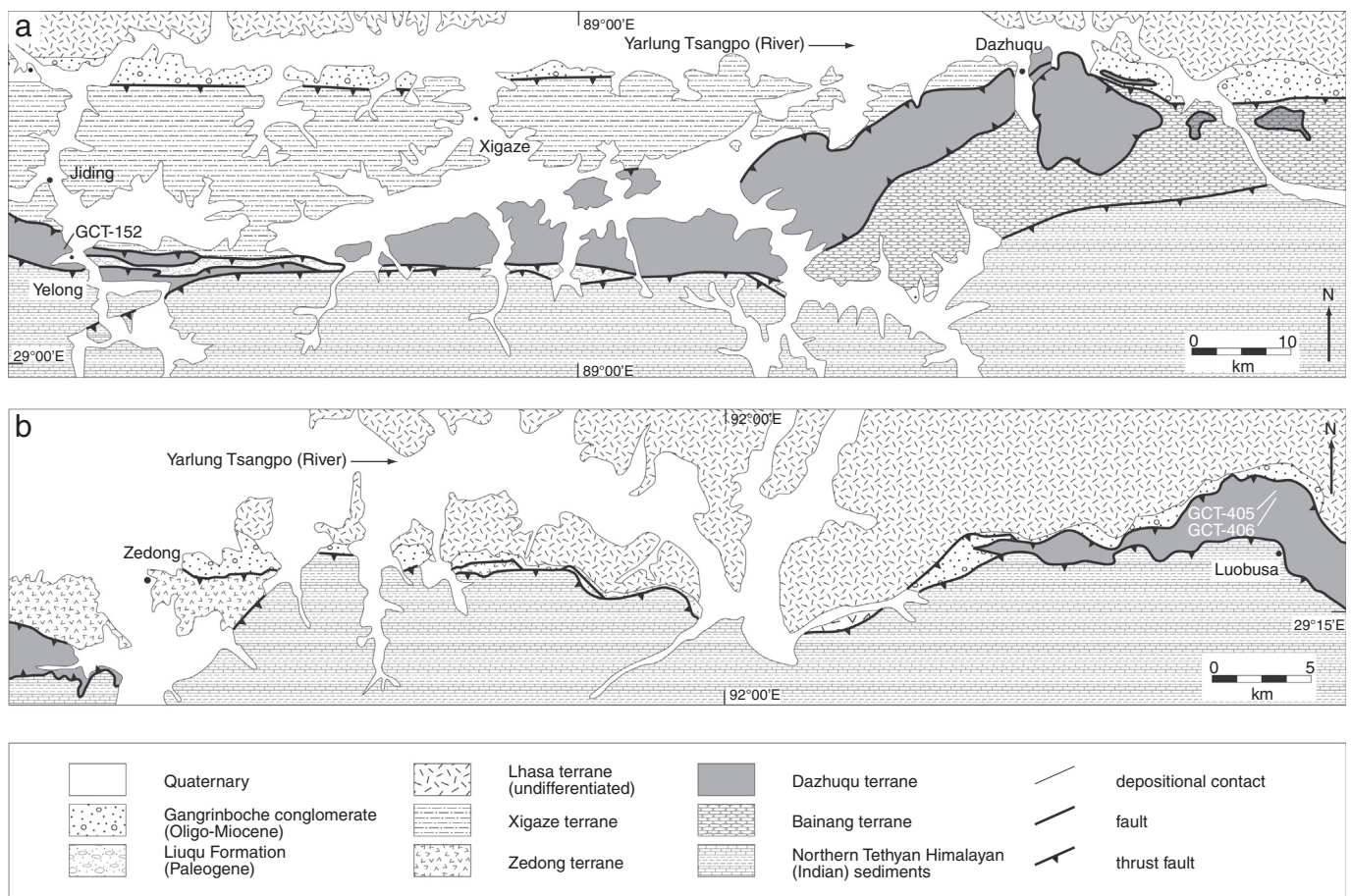


Fig. 2. Simplified geological maps of the a) Xigaze and b) Luobusa areas in the southeastern section of the YTSZ (modified after Zhou et al., 1996; Davis et al., 2002). Sites for geochronology samples are also shown.

described by Zhou et al. (1996, 2005) who argued that these rocks formed in a two-stage process. The peridotites are interpreted to represent residues of melting at a mid-ocean ridge that were subsequently modified by supra-subduction zone magmatism (Griselin et al., 1999; Zhou et al., 2005). An intra-oceanic arc was possibly created by the latter magmatic event and is likely represented by the rocks of the Zedong terrane (Aitchison et al., 2000; McDermid et al., 2002; Aitchison et al., 2007b).

The Zedong terrane is best seen near the township of Zedong, c. 40 km west of Luobusa where the whole sequence is overturned and overthrust by the Dazhuqu terrane ophiolite. In places, island arc tholeiitic pillow basalts are overlain by red ribbon cherts. This sequence is further covered by a succession of autoclastic breccias of shoshonitic affinity, which is cut locally by basaltic to dacitic dykes (McDermid et al., 2002; Aitchison et al., 2007b). It is possible that rocks assigned to Dazhuqu and Zedong terranes shared, at least in part, a common history. However, they are in faulted contact and as noted by (Hébert et al., 2012) resolution of their original relationships awaits further investigation.

A Sm–Nd age of 177 ± 31 Ma has been reported for a gabbroic dyke of the Luobusa ophiolite (Zhou et al., 2002). Ophiolitic rocks of the Zedong terrane have been more extensively dated by U–Pb ion microprobe, Ar–Ar geochronology and radiolarian biostratigraphy. The radiometric dates of the volcanic rocks and associated plutonic rocks have a wide range of 152–163 Ma whereas the chert, which overlies island arc tholeiitic pillow basalts at the base of the sequence, contains radiolarians indicative of a possible Bathonian through lower Callovian (circa 168–162 Ma; Gradstein et al., 2012) age range (McDermid et al., 2002; Aitchison et al., 2007b). Amphibolites from the melange zone structurally beneath the Luobusa ophiolite that are inferred to represent fragments

of a metamorphic sole (Malpas et al., 2003) have an Ar–Ar amphibole age of 85.7 ± 0.9 Ma and a biotite age of 80.6 ± 0.6 Ma. A further report of a 162.9 ± 2.8 Ma U/Pb zircon SHRIMP age from a diabase in the Luobusa ophiolite exists in Chinese literature (Zhong et al., 2006b).

2.3. Ophiolitic massifs in the Xigaze area

Several massifs form a near continuous ophiolite belt, stretching east–west over a distance of c. 150 km near Xigaze, SW of Lhasa (Fig. 2b). Individual massifs are up to c. 2 km thickness and collectively the belt resembles a classical complete ophiolite succession in that mantle peridotite (mainly harzburgite with minor dunite, lherzolite and wehrlite) is overlain by layered and intrusive gabbro (Nicolas et al., 1981; Girardeau et al., 1985c; Wang et al., 1987; Hébert et al., 2012; Bao et al., 2013; Dai et al., 2013). This sequence in turn passes upward to a sheeted dyke complex, which feeds pillow lavas interbedded with radiolarian chert. The ophiolite is everywhere separated from Upper Cretaceous siliciclastic turbidites of the Xigaze terrane by a late stage south-dipping, north-vergent backthrust (part of Gansser's (1964) Great Counter thrust system; Aitchison et al., 2000, 2002a; Aitchison and Davis, 2004; Aitchison et al., 2007a; cf. Wang et al., 2012). The volcanoclastic sedimentary cover of the ophiolite differs from that of the Xigaze terrane over which the ophiolite has been backthrust. It is dominated by basaltic detritus and has appreciable quantities of detrital magnetite. Where present, felsic material is concentrated in tuffaceous horizons (Ziabrev et al., 2003; Aitchison and Davis, 2004). In contrast volcanoclastic detritus in the Xigaze turbidites is dominated by material of rhyolitic to dacitic compositions (Dürr, 1996). To the south, the ophiolite lies in the footwall of a fault contact with the Tethyan

Himalayan turbidites along another strand of the north-directed Great Counter thrust system (Gansser, 1964). Although it has previously been postulated that the ophiolite formed at a MOR (Nicolas et al., 1981; Girardeau et al., 1985a), recent petrological and geochemical studies have confirmed the interpretation of Aitchison et al. (2000) that these rocks originated in a SSZ setting with both forearc and backarc affinities having been suggested (Hébert et al., 2003; Malpas et al., 2003; Dubois-Cote et al., 2005; Hébert et al., 2012; Bao et al., 2013; Dai et al., 2013).

The ophiolite has a poorly constrained U–Pb whole rock age of 120 ± 10 Ma (Göpel et al., 1984). The first published sensitive high-resolution ion microprobe (SHRIMP) U–Pb zircon age of a quartz diorite from a massif at Dazhuqu (Malpas et al., 2003) is 126 ± 2 Ma, which is consistent with another (SHRIMP) age of 128 ± 2 Ma from a gabbro another massif at Jiding (Wang et al., 2006) and 125 ± 0.88 Ma for gabbro at Qunrang (Li et al., 2009).

The inferred age range of associated basaltic volcanism is consistent with radiolarian biostratigraphy from the overlying cherts. The oldest sediments are upper Barremian (c. 127.5–125 Ma; Gradstein et al., 2012) and range through to the upper Aptian. (>112 Ma) (Ziabrev et al., 2003). Amphibolite blocks included in the sub-ophiolitic tectonic melanges, interpreted as disrupted metamorphic sole rocks, have been dated by the Ar–Ar method. Malpas et al. (2003) reported an amphibole age of 87.9 ± 0.4 Ma whereas Guilmette et al. (2009) described an older age range of 127.7 ± 2.3 – 123 ± 3.1 Ma. Paleomagnetic studies indicate that the ophiolite formed at equatorial latitudes, 1000–1500 km south of Eurasia's margin during the mid-Cretaceous (Abrajvitch et al., 2005).

2.4. Dangxiong, Jungbwa and Kiogar massifs

The southwestern Tibetan ophiolites form a 300-km-long discontinuous belt, dominated by three major massifs (from east to west): the Dangxiong, Jungbwa (Yungbwa) and Kiogar massifs (Fig. 3). These massifs occur c. 20 km to the south of the suture zone and are tectonically underlain by ophiolitic melanges. The whole package has been emplaced onto the deformed Mesozoic continental margin sequence of the north Indian plate. Late normal faulting along the southern margin of the Jungbwa massif has juxtaposed the mantle sequence rocks directly above the North Himalayan Gurla Mandata gneisses. The ophiolite has an estimated thickness of 6 km and is essentially represented by a mantle sequence, composed mainly of harzburgite with minor amounts of dunite, lherzolite and orthopyroxenite (Dai et al., 2011). Chromitite bands enveloped by dunite are also found in the Kiogar massif. Despite occasional pegmatitic gabbro dykes cutting the Jungbwa massif (Liu et al., 2010), most gabbroic rocks are found in the Dangxiong massif as layered troctolitic gabbros and isotropic gabbros (Chan, 2008). Harzburgite dominates the eastern end of the Dangxiong massif at Xiugugabu with a minor occurrence of diabase and overlying sediments (Bédard et al., 2009). The mantle and lower crustal sequences at Jungbwa are cut by basaltic, diabase and gabbroic dykes (Miller et al., 2003). A 2-km-wide shear zone occurs near the town of Laro, in which ultramafics and gabbros are mylonitized and variably metamorphosed. The gabbroic intrusions have steep foliations, which commonly parallel the fabrics observed in the mylonitic peridotites. The Jungbwa massif was the subject of a reconnaissance study by Miller et al. (2003), who suggested that the peridotites of the this massif appear to be residues of melting in a MOR, later cut by some basaltic and gabbro dykes. Miller et al. (2003) reported an Sm–Nd age of 147 ± 25 Ma and an Ar–Ar amphibole age of 152 ± 33 Ma of the basaltic dykes. A SHRIMP zircon age of 122.3 ± 2.4 Ma from the Dangxiong massif has been recently reported for diabase dikes by Wei et al. (2006). In the Jungbwa district near lakes Mapan Yum Co and La'nga Co SHRIMP zircon U/Pb ages of 118.8 ± 1.8 Ma and 120.5 ± 1.9 Ma have been reported for diabase dikes (Xia et al., 2011). Whereas (Li et al., 2008) report an age of 120.2 ± 2.3 Ma for diabase dikes south of Mapan Yum Co. LA-ICP-MS U/Pb zircon ages of 130 ± 0.5 Ma and 128 ± 1.1 Ma

have been reported from the Kiogar ophiolitic massif by Xiong et al. (2011) for pyroxenite and gabbro respectively. Ultramafic rocks in this region are generally regarded as having initial MOR origins in the Jurassic with ophiolitic rocks of Cretaceous age having formed in a SSZ intra = oceanic arc system (Miller et al., 2003; Liu et al., 2010; Dai et al., 2011).

3. Sample descriptions

Eight samples were collected from various YTSZ locations extending from east to west at: the Luobusa (GCT-405, GCT-406), Xigaze (GCT-152), Dangxiong (GCT-163, GCT-185), Jungbwa (GCT-61, GCT-134) and Kiogar (GCT-329).

3.1. Luobusa

Sample GCT-405 is a fine-grained gabbro, consisting of plagioclase, clinopyroxene with trace amounts of titanite and ilmenite. The sample was collected from a 1 m width dyke intruding serpentized dunite. Zircons in this sample are prismatic and colourless with some inclusions and range in size from $100 \times 55 \times 30$ to $50 \times 50 \times 20$ μm . Sample GCT-406 is a fine-grained gabbro, consisting of plagioclase, clinopyroxene with trace amount of titanite and ilmenite. The sample was collected from a gabbroic dyke that cuts serpentized harzburgite. The zircons are colourless or pale brown, euhedral long or stubby prisms, without any inclusions. The size of these zircons ranges from $120 \times 50 \times 30$ to $65 \times 50 \times 30$ μm .

3.2. Xigaze

Sample GCT-152 is a coarse-grained gabbro with mainly plagioclase and clinopyroxene and trace titanite, apatite and ilmenite. The sample was collected from a km-wide gabbroic stock, which is further cut by diabase dykes, to the immediate east of Yelong village. Zircons in this sample are colourless, prismatic and without any visible inclusions. The grains vary in size from $100 \times 50 \times 30$ to $70 \times 50 \times 30$ μm .

3.3. Dangxiong

Sample GCT-185 from is a coarse-grained gabbro, comprising plagioclase, clinopyroxene and trace amount of quartz, apatite, magnetite and ilmenite. The sample was collected from a 500 m width gabbro stock, to the southwest of Laro village. Zircons in this sample are colourless, pale brown, euhedral or fragmentary and range in size from $90 \times 50 \times 40$ to $40 \times 35 \times 20$ μm . Sample GCT-163 is a coarse-grained gabbro composed of plagioclase, clinopyroxene with trace titanite, apatite and ilmenite. The sample was collected from a 20 cm thick dyke that cuts fine-grained gabbro to the immediate west of Laro village. Zircons of similar colour and morphology to those in GCT-185 were found, but they range in size from $160 \times 35 \times 20$ to $50 \times 50 \times 20$ μm .

3.4. Jungbwa

Sample GCT-134 is a medium-grained gabbro, consisting of plagioclase, clinopyroxene, and hornblende, with minor apatite and ilmenite. The sample was collected from a stock several hundred meters wide that intrudes serpentized harzburgite of the Jungbwa massif. Zircon grains from the gabbro are colourless to pale brown and typically subhedral prismatic with sizes ranging from $90 \times 45 \times 40$ to $50 \times 30 \times 20$ μm . Sample GCT-61 from Jungbwa is a coarse-grained gabbro, composed of plagioclase, clinopyroxene, orthopyroxene and trace amount of apatite. The sample was collected from a 30 cm wide dyke that crosscuts serpentized harzburgite in the southern part of the Jungbwa massif. Very few zircons were separated from this sample. They are colourless, anhedral prismatic grains $80 \times 40 \times 40$ μm .

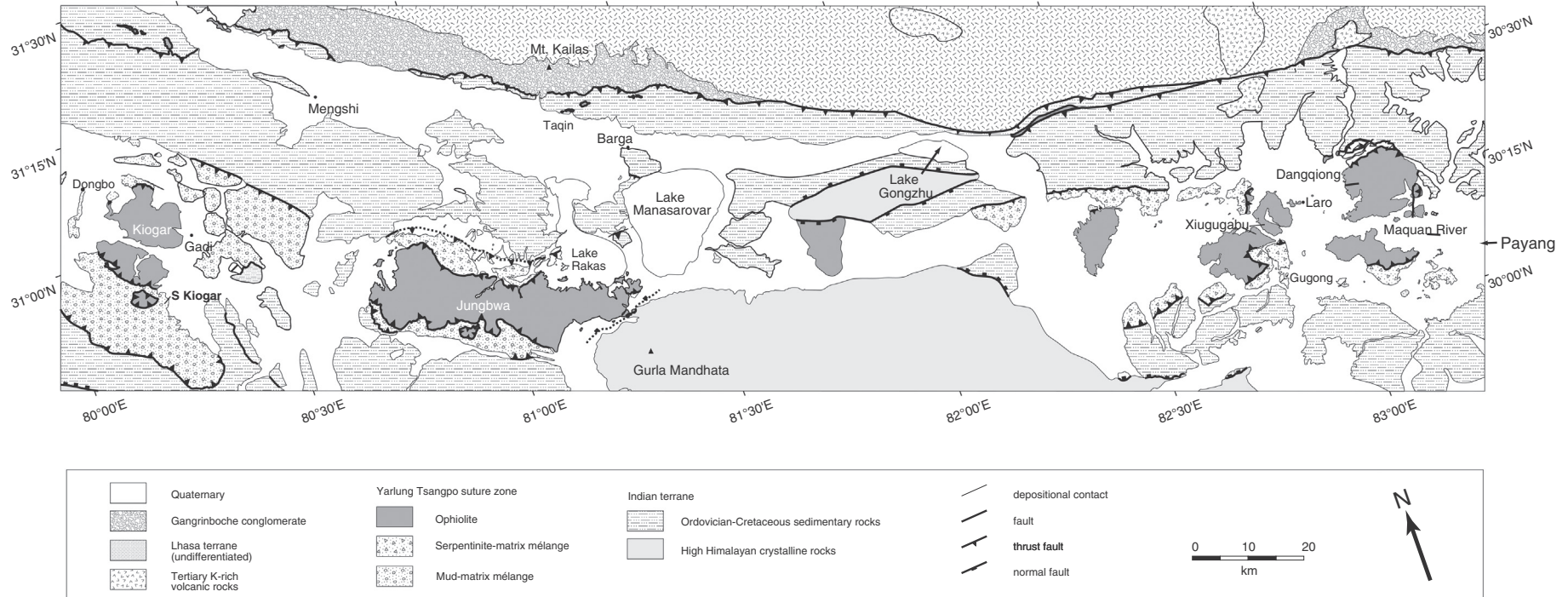


Fig. 3. Simplified geological map of the southwestern section of the YTSZ, showing the Dongxiang, Jungbwa and Kiogar massifs (after Guo et al., 1991), field mapping and satellite imagery interpretations.

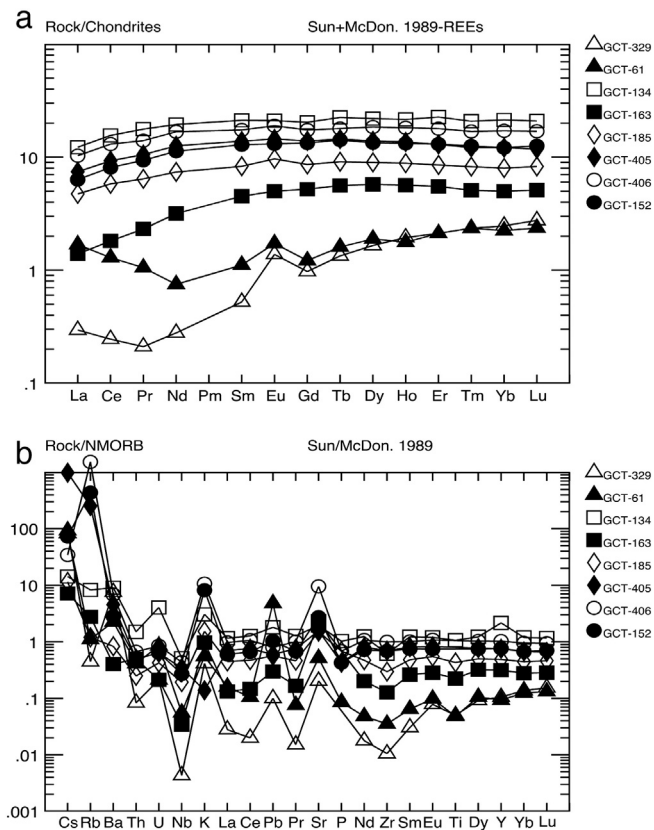


Fig. 4. (a) MORB- and (b) chondrite-normalized diagrams of the dated samples.

3.5. Kiogar

Sample GCT-329 is an extremely coarse-grained gabbronorite (grain size up to 5 cm), comprising plagioclase, orthopyroxene and clinopyroxene. The sample was collected from a ~5 m wide intrusive body that cuts harzburgite, ~2 km west of Gadi village (Fig. 4). Almost 10 kg of sample was crushed, sieved and separated, but only one zircon was found. The zircon is fragmentary ($50 \times 45 \times 20 \mu\text{m}$), colourless, without any visible inclusions.

4. Sample geochemistry

Geochemical analyses of all the dated samples were performed at the University of Hong Kong. Major element abundances were determined using X-ray fluorescence (XRF) on fused glass. The trace elements Sc, V, Cr, Ni, Cu, and Zn were also determined by XRF on pressed powder pellets. The remaining trace elements and the rare earth elements (REE) presented in Table 1 were determined on a VG Elemental Plasma-mass spectrometer (ICP-MS). The protocol of Jenner et al. (1991), with standard additions, pure elemental standards for external calibration, and international standard BHVO-1 taken as reference sample was used. Accuracies of the XRF analyses are estimated as $\pm 2\%$ for major elements present in concentrations greater than 0.5-wt.% and $\pm 5\%$ for trace elements. The ICP-MS results were obtained with accuracy better than $\pm 5\%$.

Similar geochemical features characterize all gabbros from the various ophiolite localities. On the N-MORB normalized diagram (Fig. 4), they all display relative low contents of Nb, Zr and variable alkalis, Rb, Ba, Th, U and Sr relative to MORB. In contrast, the gabbronorites from the Kiogar and Jungbwa massifs are much depleted (0.003–0.1 times N-MORB values) and display pronounced negative anomalies in Nb

and Zr and positive anomalies in Sr and Eu. The chondrite-normalized REE patterns of the gabbros show light REE (LREE) depletion, spanning the range of typical MORB. Patterns of the gabbronorites from the Kiogar and Jungbwa massif are lower than the typical MORB composition and show enrichment in LREE.

The gabbros show enrichment in large ion lithophile elements relative to MORB, clear Nb depletion and similar high field strength element to MORB. All these lines of evidence suggest that they were generated in a SSZ environment. The spoon-shaped REE element patterns of the gabbronorites are comparable with boninitic gabbros elsewhere (e.g. the Trinity ophiolite in California; Metcalf et al., 2000), although these rocks are probably cumulate and their whole-rock compositions might not approximate to the primary magma. However, it is important to note that the occurrence of orthopyroxene and crystallization of plagioclase after pyroxenes in these rocks differs from those formed at MOR. We favour an interpretation that the gabbronorites crystallized from boninitic magmas in a SSZ setting.

Further details and detailed discussion of the petrogenesis and geochemistry of ophiolitic rocks along the YTSZ are presented in numerous recent works (Hébert et al., 2003; Zhou et al., 2005; Zhong et al., 2006a; Guilmette et al., 2009; Dai et al., 2011; Hébert et al., 2012; Bao et al., 2013; Dai et al., 2013).

5. U/Pb dating

5.1. Methodology

Ages were determined by either isotope dilution thermal ionization mass spectrometry (ID-TIMS) or laser ablation multi-collector inductively coupled plasma mass spectrometry (LA-MC-ICP-MS) at the NERC Isotope Geosciences Laboratory (NIGL), Keyworth, UK. Data and errors were calculated using the Isoplot 3 macro of Ludwig (2003). The final data (2σ error ellipses) are plotted in Fig. 5. Detailed analytical data coupled with the coordinates of sample localities are presented in Tables 2A and 2B.

Zircons were separated from the rock samples using standard separation techniques (Rogers water table, Frantz magnetic separation, and MI heavy-liquid separation). For U–Pb ID-TIMS, selected grains were chemically abraded to minimize possible Pb-loss using a modified chemical abrasion technique of Mattinson (2005). This involved annealing bulk zircon fractions at 800 °C in quartz glass beakers for 48 hours. The zircon crystals were subsequently cleaned ultrasonically in 4 N HNO₃, rinsed in ultra-pure water, then further washed in warm 4 N HNO₃ prior to rinsing with distilled water to remove surface contamination. The annealed, cleaned bulk zircon fractions were then chemically leached in 200 μl 29 N HF and 20 μl 8 N HNO₃ at 120 °C for 12 hours. Chemically abraded zircons were washed several times in ultra-pure water, cleaned in warm 4 N HNO₃ for several hours on a hot-plate, rinsed again in ultra-pure water and 8 N HNO₃ and split into single grain fractions ready for dissolution. Three samples were analysed by LA-MC-ICP-MS. These samples were embedded into epoxy mounts and surface polished to expose an equatorial section through the crystals.

For U–Pb chemistry prior to TIMS analysis, the recently calibrated EARTHTIME mixed ²⁰⁵Pb/²³⁵U tracer was used to spike all fractions. Dissolved, spike equilibrated samples were not subjected to ion-exchange procedures but were converted to chloride and loaded onto degassed rhenium filaments in silica gel following a procedure modified after Mundil et al. (2004). Analyses were performed using a Thermo Electron Triton equipped with a new generation of MassCom Secondary Electron Multiplier (Noble et al., 2006). A minimum of 100 ratios were collected for Pb and 60 for U. Pb ratios were scrutinised for any evidence of organic interferences which were determined to be negligible. Total procedural blanks for three separate batches of chemistry between October 2004 and April 2006 were 2.0

Table 1
Major and trace element compositions of the dated samples.

Location	Kiogar	Jungbwa	Jungbwa	Dangxiong	Dangxiong	Luobusa	Luobusa	Xigaze
Sample no.	GCT-329 gabbronorite	GCT-61 gabbronorite	GCT-134 gabbro	GCT-163 gabbro	GCT-185 gabbro	GCT-405 diabase	GCT-406 diabase	GCT-152 gabbro
<i>Major oxides (wt%)</i>								
SiO ₂	49.69	47.59	46.24	48.69	48.91	46.81	49.12	48.95
TiO ₂	0.06	0.06	1.35	0.28	0.55	0.87	1.23	0.90
Al ₂ O ₃	12.29	19.23	15.55	17.94	18.92	15.20	15.38	15.87
Fe ₂ O ₃	5.31	3.22	11.35	3.95	6.09	8.79	9.97	8.31
MnO	0.11	0.06	0.19	0.09	0.11	0.15	0.15	0.15
MgO	15.90	11.83	6.51	8.05	6.31	7.70	6.86	7.62
CaO	12.59	15.26	11.88	14.64	13.44	12.98	10.51	11.48
Na ₂ O	0.35	0.44	2.25	2.42	2.17	2.75	2.82	2.64
K ₂ O	0.03	0.04	0.22	0.07	0.11	0.01	0.77	0.59
P ₂ O ₅	0.00	0.01	0.12	0.00	0.08	0.05	0.08	0.05
LOI	2.26	1.53	3.97	3.07	2.43	3.53	2.37	2.70
TOTAL	98.60	99.28	99.62	99.22	99.11	98.83	99.26	99.24
<i>Trace elements (ppm)</i>								
Ti	381	366	8112	1701	3281	–	–	–
Sc	48.2	29.2	35.2	42.8	34.0	45.16	28.42	38.37
Rb	0.25	0.62	4.62	1.54	0.67	141.30	857.55	244.70
Sr	18.3	46.3	175	207	136	141.30	857.55	244.70
Y	2.95	2.62	60.41	8.83	13.7	21.07	28.77	21.42
Zr	0.78	2.61	45.66	9.42	22.0	51.43	73.86	50.96
Nb	0.01	0.13	1.20	0.08	0.45	0.80	1.02	0.63
Cs	0.65	0.58	0.10	0.05	0.08	6.88	0.24	0.51
Ba	47.5	14.2	56.9	2.56	5.25	28.52	42.97	17.66
Ta	–	0.10	0.03	–0.03	0.01	0.04	0.10	0.02
Hf	0.03	0.53	1.98	0.35	0.71	1.43	2.10	1.42
Pb	0.03	1.43	0.54	0.09	0.17	0.18	0.24	0.31
Th	0.01	0.05	0.18	0.06	0.03	0.06	0.08	0.06
U	0.01	0.04	0.19	0.01	0.02	0.03	0.04	0.03
V	185	141	–	143	204	174.10	216.92	459.10
Cr	593	749	–	417	204	47.23	78.94	113.25
Ni	505	340	–	103	204	39.73	69.03	71.14
Cu	14.4	8.29	–	3.34	204	41.42	41.98	52.82
Zn	26.9	26.7	–	16.1	204	217.24	263.89	225.02
La	0.07	0.40	2.90	0.33	1.12	1.76	2.44	1.50
Ce	0.15	0.79	9.53	1.11	3.55	5.68	7.99	4.96
Pr	0.02	0.10	1.68	0.22	0.61	1.00	1.33	0.89
Nd	0.13	0.35	9.08	1.48	3.45	5.88	7.83	5.27
Sm	0.08	0.17	3.24	0.69	1.27	2.12	2.66	1.97
Eu	0.08	0.10	1.22	0.29	0.56	0.84	1.10	0.76
Gd	0.20	0.25	4.18	1.07	1.77	2.86	3.57	2.74
Tb	0.05	0.06	0.84	0.21	0.34	0.54	0.67	0.53
Dy	0.42	0.48	5.57	1.46	2.28	3.53	4.69	3.41
Ho	0.11	0.10	1.22	0.32	0.50	0.77	1.03	0.75
Er	0.35	0.35	3.75	0.91	1.41	2.14	2.96	2.16
Tm	0.06	0.06	0.53	0.13	0.21	0.31	0.43	0.32
Yb	0.42	0.38	3.63	0.85	1.36	2.06	2.91	2.06
Lu	0.07	0.06	0.53	0.13	0.21	0.30	0.43	0.32

to 0.2 pg for Pb and 0.3 to 0.1 pg for U. Samples were blank corrected using the ²⁰⁴Pb:²⁰⁶Pb:²⁰⁷Pb:²⁰⁸Pb ratio measured during the analysis (1: 18.70:15:15:36.82). Correction for common lead in all samples was carried out using the Stacey and Kramers (1975) common lead evolutionary model.

Laser ablation geochronology was conducted following the procedures of Simonetti et al. (2005) and Horstwood et al. (2003). This included the use of the 91500 zircon as a primary standard. For each analytical session the overall reproducibility of the primary standard ²⁰⁶Pb/²³⁸U was in the order of 2–3% (2σ), this has been propagated into the uncertainties for each analysis. A fast-washout ablation cell was used to increase the time-resolution of the data. Measurements used a Nu-Plasma HR MC-ICP-MS coupled with a New Wave Research LUV266X Nd:YAG laser ablation system. The grains were ablated using a 20- or 35-μm-diameter spot or 20-μm-wide line raster depending on the size of the crystal. A ²⁰⁵Tl/²³⁵U solution was simultaneously aspirated during analysis to correct for instrumental mass bias and plasma-induced inter-element fractionation using a Cetac Technologies Aridus desolvating nebulizer. Ages and errors were calculated using the Isoplot 3 macro of Ludwig (2003).

5.2. Results

5.2.1. Luobusa

Five analyses were conducted on zircons from sample GCT-405 using LA-MC-ICP-MS and the results are plotted in a Tera–Wasserburg diagram (Fig. 5a). These data form an array with an intercept age of 148.6 ± 4.2 Ma (MSWD = 0.69). The same analyses give a weighted mean ²⁰⁶Pb/²³⁸U age of 148.4 ± 4.5 Ma. The age of sample GCT-406 was also determined by LA-MC-ICP-MS. Six data points form a concordant cluster with a weighted mean ²⁰⁶Pb/²³⁸U age of 149.9 ± 2.2 Ma (MSWD = 0.42) (Fig. 5b).

5.2.2. Xigaze

Sample GCT-152 was dated by LA-MC-ICP-MS. Ten analyses yielded a concordant cluster with a weighted mean ²⁰⁶Pb/²³⁸U age of 131.8 ± 1.3 Ma (MSWD = 0.60) (Fig. 5c).

5.2.3. Dangxiong

Five single-grain fractions from sample GCT-185 were analysed by TIMS and yielded a concordia age of 126.69 ± 0.41 Ma and a weighted

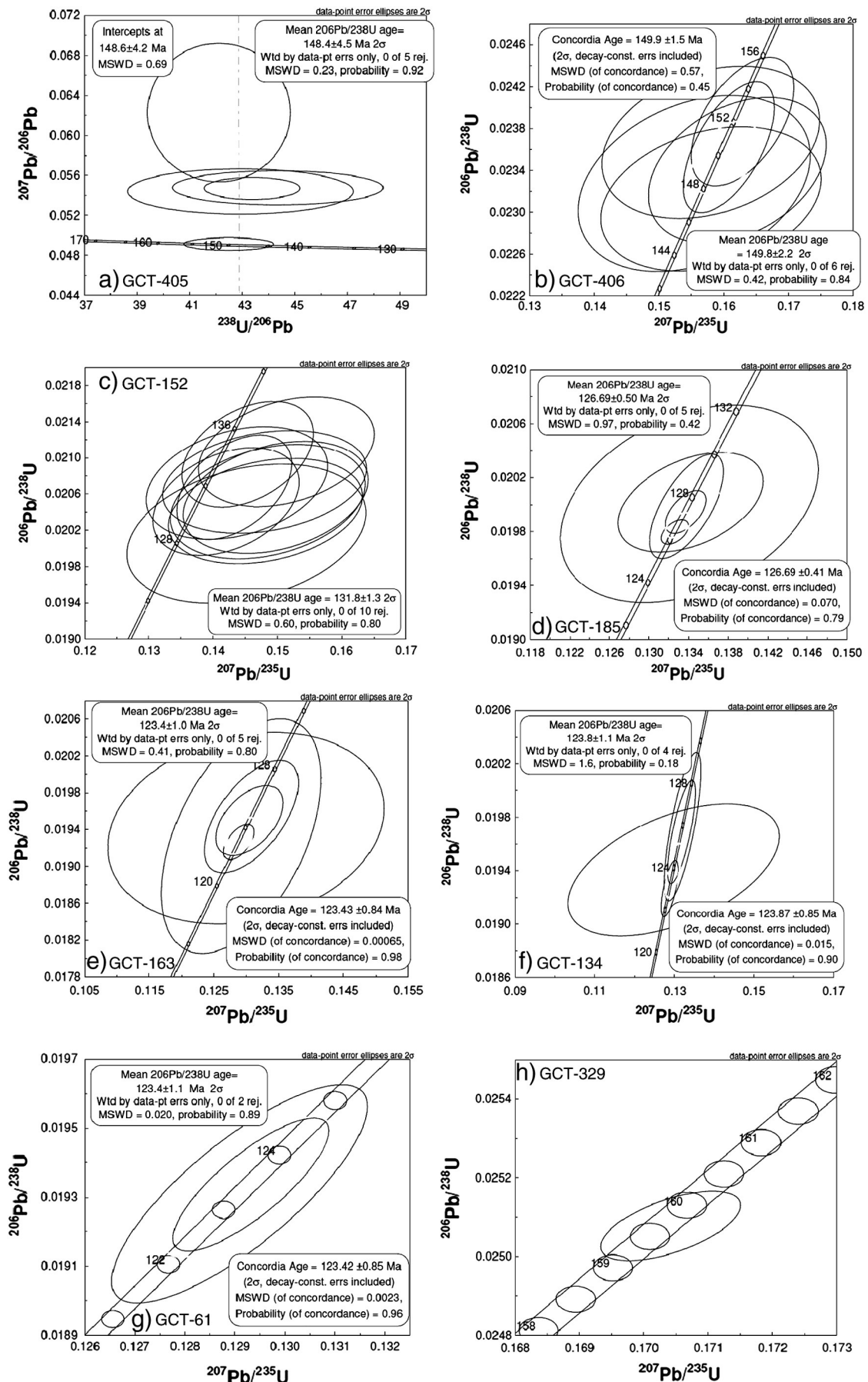


Fig. 5. U–Pb concordia and Tera–Wasserberg diagrams showing the data points for samples analysed by LA-MC-ICP-MS and TIMS.

Table 2A
LA-MC-ICPMS U–Pb data.

	U (ppm)*	Isotopic ratios†						Ages (Ma)						
		²⁰⁷ Pb/ ²⁰⁶ Pb	2σ%	²⁰⁶ Pb/ ²³⁸ U	2σ%	²⁰⁷ Pb/ ²³⁵ U	2σ%	Rho‡	²⁰⁷ Pb/ ²⁰⁶ Pb	2σ abs	²⁰⁶ Pb/ ²³⁸ U age	2σ abs	²⁰⁷ Pb/ ²³⁵ Pb age	2σ abs
<i>GCT-405, Luobusa N 29.22807° E 92.17838° diabase</i>														
z4	1127.9	0.0548	2.5	0.0225	7.4	0.170	7.8	0.95	402.8	56.8	143.7	10.7	159.7	13.4
z5	425.7	0.0623	9.1	0.0237	5.3	0.204	10.5	0.50	683.7	193.7	151.3	8.0	188.4	21.5
z6	523.9	0.0544	3.4	0.0233	8.2	0.175	8.8	0.92	387.5	76.5	148.4	12.2	163.5	15.6
z7	1515.3	0.0491	1.1	0.0235	3.3	0.159	3.4	0.95	154.6	24.9	150.0	5.0	150.2	5.5
z8	506.1	0.0547	1.6	0.0231	3.4	0.174	3.8	0.90	400.5	36.9	146.9	5.1	162.8	6.7
<i>GCT-406, Luobusa N 29.23117° E 92.18645° diabase</i>														
z1	880.8	0.0502	6.5	0.0234	2.4	0.162	6.9	0.35	206.1	150.5	149.1	3.7	152.5	11.3
z3	626.4	0.0496	8.5	0.0231	2.4	0.158	8.8	0.28	174.1	197.7	147.4	3.6	149.0	14.0
z5	550.5	0.0484	9.0	0.0233	3.0	0.155	9.4	0.31	120.3	211.4	148.3	4.4	146.7	14.8
z6	660.1	0.0484	8.3	0.0237	2.5	0.158	8.7	0.29	119.6	196.6	150.8	3.8	148.9	13.9
z14	1050.1	0.0494	2.8	0.0236	2.2	0.161	3.6	0.61	165.4	66.3	150.5	3.3	151.4	5.8
z16	1099.1	0.0495	3.4	0.0239	2.1	0.163	4.0	0.53	172.1	78.5	152.0	3.2	153.3	6.5
<i>GCT-152, Xigaze N 29.13193° E 88.38178° coarse grained gabbro</i>														
z3	151.0	0.0522	10.0	0.0202	3.1	0.145	10.5	0.30	294.1	228.3	128.7	4.0	137.6	15.3
z7	441.6	0.0501	5.3	0.0210	2.3	0.145	5.7	0.40	200.0	122.1	134.2	3.1	137.8	8.4
z8	356.4	0.0502	6.1	0.0205	2.4	0.142	6.5	0.36	204.1	141.2	130.9	3.1	134.8	9.4
z9	237.2	0.0503	7.6	0.0207	2.5	0.144	8.0	0.31	208.3	176.7	132.2	3.3	136.3	11.6
z10	600.8	0.0503	4.5	0.0207	2.3	0.143	5.1	0.45	207.1	105.3	131.9	3.0	136.0	7.4
z11	192.3	0.0518	8.4	0.0207	2.2	0.148	8.7	0.26	274.9	193.3	132.3	3.0	140.1	13.0
z12	216.8	0.0525	7.9	0.0205	2.5	0.148	8.3	0.30	306.7	180.6	130.9	3.3	140.6	12.5
z15	243.9	0.0528	7.4	0.0206	2.5	0.150	7.8	0.31	320.1	169.0	131.2	3.3	141.6	11.8
z16	215.4	0.0526	8.0	0.0204	2.3	0.148	8.3	0.28	312.6	181.4	130.3	3.1	140.2	12.4
z17	259.5	0.0521	7.0	0.0211	2.4	0.151	7.4	0.32	290.0	159.4	134.4	3.2	143.1	11.3

* Accuracy of U concentration is ~10%.

† All isotopic ratios are non-common-Pb corrected.

‡ Error correlation coefficient calculated using isoplot (Ludwig, 2003).

mean ²⁰⁶Pb/²³⁸U age of 126.69 ± 0.50 Ma (Fig. 5d). Five single-grain fractions from sample GCT-163 were also analysed by TIMS and produced a concordia age of 123.43 ± 0.84 Ma and a weighted mean ²⁰⁶Pb/²³⁸U age of 123.4 ± 1.0 Ma (Fig. 5e).

5.2.4. Jungbwa

Four single-grain fractions from sample GCT-134 were analysed by TIMS and yielded a concordia age of 123.87 ± 0.85 Ma and a weighted mean ²⁰⁶Pb/²³⁸U age of 123.8 ± 1.1 Ma (Fig. 5f). Two single-grain fractions from sample GCT-61 were also analysed by TIMS and overlap within error to give a concordia age of 123.42 ± 0.85 Ma and a weighted mean ²⁰⁶Pb/²³⁸U age of 123.4 ± 1.1 Ma (Fig. 5g).

5.2.5. Kiogar

The age of sample GCT-329 was determined by TIMS. The only fraction gives a concordant ²⁰⁶Pb/²³⁸U age of 159.7 ± 0.5 Ma (Fig. 5h), which it taken as a tentative magmatic age for the sample.

5.3. Interpretation

The mantle peridotites at Luobusa are essentially residues from melting at a MOR, subsequently modified by SSZ magmatism (Bai et al., 1993; Zhou et al., 1996, 2005). The dated gabbros (c. 150 Ma.) display a SSZ geochemical signature and are therefore likely to have formed during a later stage of magmatism. This age postdates, or partly overlaps within error of the age range of volcanic rocks (163–152 Ma) exposed in the Zedong terrane (McDermid et al., 2002; Aitchison et al., 2007b). These dated volcanic rocks overlie late Middle Jurassic island arc tholeiites and overlying cherts and were erupted during intra-arc rifting (Aitchison et al., 2007b). The relationships between the Luobusa and Zedong terranes remain conjectural as all contacts are faulted, but Aitchison et al. (2007b) envisaged that the Zedong terrane developed during intra-arc rifting, which pre-dates formation of gabbros dated in this study. Hence this raises a possibility that continued rifting led to breakup of the arc and formation of a basin in the backarc region, into which these gabbroic dykes invaded.

The gabbro from the Xigaze ophiolite has an age of 131.8 ± 1.3 Ma, which is slightly older than those previously reported (126 ± 2 Ma from a quartz diorite at Dazhuqu; Malpas et al. (2003) and 128 ± 2 Ma from a gabbro at Jiding; Wang et al. (2006)). Combining available geochronological and biostratigraphic data (Ziabrev et al., 2003) this suggests the SSZ magmatism may have lasted from 132–126 Ma. In southwest Tibet, the U–Pb ages of the gabbroic rocks from the Dangxiong ophiolite, range from 127 to 123 Ma, which is consistent with an age of 122.3 ± 2.4 Ma for a diabase from along strike (Wang et al., 2006). The crustal rocks of the Jungbwa ophiolite formed in a similar time frame. The gabbro has an age of 123.42 ± 0.85 Ma, which is indistinguishable from the age of the gabbro from the same massif (123.87 ± 0.85 Ma). The gabbro exhibits a LREE-enriched boninite-like signature in contrast to SSZ-tholeiitic signature recorded by the gabbro. The concomitant ages are interpreted to reflect the co-genetic formation of these two suites of rocks in a SSZ setting.

6. Discussion

By the early Middle Jurassic >4000 km of Neo-Tethyan Ocean separated Eurasia from India, which was then still part of Gondwana (Besse and Courtillot, 1988). A series of northwest-southeast trending spreading ridges are postulated to have developed to the north of the Indian passive margin, facilitating formation of MORB-type oceanic lithosphere (Besse and Courtillot, 1988). A segment of this oceanic lithosphere may be represented by a present-day volumetrically dominant tholeiitic suite of the Spontang ophiolite in Ladakh and perhaps the depleted MORB-type peridotites preserved at Jungbwa and Luobusa in southern Tibet.

Commencing in the Late Jurassic, the motions of the plates bordering Neo-Tethys changed considerably. This may have been associated with rifting of Argo-Burma terrane from NW Australia (Stampfli and Borel, 2002; Gibbons et al., 2012) and the rifting of India from Africa (Coffin and Rabinowitz, 1987; Ali and Aitchison, 2008). Plate reorganization possibly induced the formation of a north-dipping intra-oceanic subduction zone, located around the equatorial region (Abrajevitch et al.,

Table 2B
TIMS U–Pb data.

	weight (μg)	U(ppm)	Pb(ppm) [†]	Pb (pg) [‡]	Isotopic ratios						Ages (Ma)							
					²⁰⁶ Pb/ ²⁰⁴ Pb [§]	²⁰⁷ Pb/ ²⁰⁶ Pb [¶]	2σ (%)	²⁰⁶ Pb/ ²³⁸ U [¶]	2σ (%)	²⁰⁷ Pb/ ²³⁵ U [¶]	2σ (%)	Rho [⌞]	²⁰⁷ Pb/ ²⁰⁶ Pb	2σ (Ma)	²⁰⁶ Pb/ ²³⁸ U	2σ (Ma)	²⁰⁷ Pb/ ²³⁵ U	2σ (Ma)
<i>The Dangxiong massif, GCT-185, N 30.23942° E 82.89673° coarse grained gabbro</i>																		
z1-1*	4.2	181.7	10.6	17.8	69.2	0.04859	0.7	0.01980	0.4	0.13262	0.8	0.50	128.0	17.1	126.4	0.5	126.4	1.1
z1-3	0.5	516.5	29.6	8.2	54.7	0.04856	1.7	0.01999	1.6	0.13381	2.3	0.67	126.5	39.9	127.6	2.0	127.5	3.1
z1-4	1.6	41.8	5.4	8.5	33.4	0.04862	4.1	0.02002	1.5	0.13419	4.5	0.42	129.6	95.7	127.8	1.9	127.9	6.1
z1-5	1.0	52.8	8.4	8.4	31.7	0.04861	7.4	0.02000	3.0	0.13407	7.9	0.35	129.0	175.3	127.7	3.9	127.8	10.8
z2-1*	4.1	175.7	7.2	12.3	83.5	0.04862	1.0	0.01995	0.7	0.13370	1.2	0.56	129.5	24.2	127.3	0.8	127.4	1.7
<i>The Dangxiong massif, GCT-163, N 30.28087° E 82.92470° coarse grained gabbro</i>																		
z1-1*	6.1	0.0	0.0	0	51.6	0.04849	1.2	0.01926	0.8	0.12880	1.5	0.57	123.3	28.9	123.0	1.0	123.0	1.9
z1-2*	1.6	0.0	0.0	0	28.1	0.04853	13.3	0.01942	4.4	0.12992	13.4	0.20	125.2	312.3	124.0	5.5	124.0	17.6
z1-4	0.7	0.0	0.0	0	38.6	0.04853	3.6	0.01954	2.6	0.13076	4.5	0.60	125.3	85.6	124.7	3.2	124.8	6.0
z1-5	0.5	0.0	0.0	0	39.8	0.04848	7.0	0.01933	5.4	0.12920	7.8	0.49	122.7	164.8	123.4	6.7	123.4	10.2
z2-1*	3.7	0.0	0.0	0	40.4	0.04853	2.8	0.01950	1.6	0.13047	3.2	0.50	125.2	66.1	124.5	2.0	124.5	4.3
<i>The Jungbwa massif, GCT-134, N 30.56662° E 81.31613° medium grained gabbro</i>																		
z1-1	1.2	0.0	0.0	0	56.9	0.04855	1.9	0.01973	2.3	0.13208	2.8	0.75	126.4	44.4	125.9	2.9	126.0	3.8
z1-2*	0.8	0.0	0.0	0	24.0	0.04852	16.7	0.01941	2.1	0.12982	16.7	0.51	124.6	393.6	123.9	2.6	123.9	21.8
z1-3	0.6	0.0	0.0	0	70.8	0.04850	1.0	0.01927	0.9	0.12883	1.3	0.67	123.6	23.6	123.0	1.1	123.0	1.8
z2-1	0.8	0.0	0.0	0	62.1	0.04855	1.4	0.01969	1.6	0.13180	2.2	0.76	126.0	33.1	125.7	2.0	125.7	2.9
<i>The Jungbwa massif, GCT-61, N 30.59481° E 81.28422° coarse grained gabbro</i>																		
z1-1*	1.0	0.0	0.0	0	84.1	0.04849	1.0	0.01931	1.3	0.12909	1.6	0.80	123.1	22.9	123.3	1.7	123.3	2.1
z1-2	1.5	0.0	0.0	0.0	111.0	0.04850	0.6	0.01934	0.8	0.12932	1.0	0.81	124.0	13.6	123.5	1.0	123.5	1.3
<i>The Kiogar massif, GCT-329, N 31.03797° E 80.29572° coarse grained gabbro</i>																		
z1-1	0.8	0.0	0.0	0	112.4	0.04929	0.4	0.02508	0.3	0.17042	0.5	0.60	161.4	9.8	159.7	0.5	159.8	0.9

* Samples not being subjected to ion-exchange procedures.

† Radiogenic lead corrected for mass fractionation, laboratory Pb, spike and initial common Pb.

‡ Total common Pb.

§ ²⁰⁶Pb/²⁰⁴Pb is a measured ratio corrected for mass fractionation and common lead in the ²⁰⁵Pb/²³⁵U spike.

¶ Corrected for mass fractionation, laboratory Pb & U spike and initial common Pb.

⌞ Error correlation coefficient calculated using isoplot (Ludwig, 2003).

2005). Much of the existing Early Jurassic or early oceanic lithosphere was subducted along this intra-oceanic island arc system. During continued subduction, an intra-oceanic island arc, represented by the Zedong terrane formed in the latest Mid Jurassic. This was locally followed by intra-arc rifting during which rocks of shoshonitic affinity were erupted (Aitchison et al., 2007b). Extension induced formation of a basin, in which SSZ-type gabbroic rocks intruded the Luobusa depleted, MORB-type, peridotites at c. 150 Ma. The temporal extent of this intra-oceanic subduction system is uncertain, but a north-dipping subduction zone appears to have developed further to the west between c. 132–123 Ma. As the dense older oceanic lithosphere was consumed at the subduction zone, roll back of the subducting slab ensued, with southward migration of the trench and consequent extension of the overriding plate. Extensional tectonics induced formation of SSZ-type ophiolites at spreading centers above the subduction zones. Blocks of amphibolites occurring in the sub-ophiolitic mélanges may be derived from the metamorphic soles, suggesting initial displacement of these ophiolites between c. 128–123 Ma (Guilmette et al., 2009).

Other Mesozoic ophiolitic rocks associated with this belt extend from Nagaland in NE India across southern Tibet and into NW India at Nidar and Spontang, thence Pakistan at Waziristan and Muslim Bagh. Superficially they resemble classical ophiolites in that peridotite, gabbro and basalt interlayered with radiolarian chert, are all present (Corfield et al., 2001; Mahéo et al., 2004). In NW India upper Barremian-mid Aptian radiolarians have been recovered from the sediments intercalated with the basalts of the Nidar ophiolite, providing an inferred age of the associated SSZ-type basaltic magmatism (Mahéo et al., 2004; Zybrev et al., 2008). The Spontang ophiolite has a U–Pb zircon age of 177 ± 1 Ma (Pedersen et al., 2001) and is overlain by Lower Cretaceous radiolarian chert (Baxter et al., 2010) and a Late Cretaceous andesitic arc sequence at 88 ± 5 Ma (Spong arc; Pedersen et al., 2001). Corfield et al. (2001) interpreted the ophiolite as representing Jurassic Tethyan MORB crust with a Late Cretaceous island arc, built on it during initiation of the subduction–obduction process.

In the Late Cretaceous, rapid northward movement of the Indian plate (Besse and Courtillot, 1988) was possibly accommodated by the formation of other subduction zone systems, one of which was located in northern regions of the Neo-Tethyan Ocean. This additional intra-oceanic island arc system formed closer to the Eurasian margin and included the Kohistan island arc, which initiated during the Jurassic with an important phase of convergence between 99 and 82 Ma; (Schaltegger et al., 2002), and was subsequently accreted to the Eurasian plate (see Burg, 2011 for a detailed discussion). Another north-dipping subduction zone is also inferred to have developed, extending from the north of the Arabian passive margin to the Indian passive margin. The Late Cretaceous Semail ophiolite in Oman/UAE and the Spong arc sequence perhaps developed in this supra-subduction zone, with the Semail ophiolite obducted onto the Arabian continental margin in the latest Cretaceous (e.g. Searle and Cox, 1999; Corfield et al., 2001; Goodenough et al., 2010). 88–80 Ma metamorphic sole rocks in southern Tibet may be counterparts of those now preserved in Oman and the UAE (Searle and Malpas, 1982; Hacker, 1994; Hacker and Gnos, 1997; Styles et al., 2006), which developed during the initial displacement of the Semail ophiolite.

Obduction of ophiolitic rocks onto the Indian northern margin occurred as oceanic lithosphere between the margin and the intra-oceanic subduction zone was completely consumed. Searle and Treloar (2010) noted that in Ladakh and Zaskar most of the crustal shortening and extreme thickening of Mesozoic shelf carbonates occurred prior to deposition of unconformably overlying Paleocene–Eocene shallow marine carbonates. Using Oman as an analogy, they suggested that this deformation resulted from the Late Cretaceous obduction of the Spontang ophiolite onto the passive margin of India.

In southern Tibet it is less possible to be certain about the precise timing of ophiolite obduction as evidence for such an event appears to be paradoxical. However, it would seem likely that all ophiolites along

the Himalaya were emplaced during an event that could have spanned ~20 million years. One thing that appears certain is that if indeed these rocks were part of an intra-oceanic (intra Tethyan) island arc system they must have collided with either India or Eurasia before the two continents collided and the Tethyan Ocean closed once and for all. All available structural evidence and detrital sedimentology indicate emplacement was onto the northern margin of India rather than southern Eurasia.

High-grade amphibolitic rocks found in mélangé zones beneath the base of ophiolitic successions have been widely interpreted as timing of initial oceanic lithosphere displacement and emplacement. Such rocks have been found from the mélangé zones at Xigaze and Luobusa. In the former area, most of the metamorphic sole rocks have ages of 128–123 Ma (Guilmette et al., 2009) whereas a much younger block of (88 Ma) amphibolite was also found (Malpas et al., 2003). Similar Late Cretaceous amphibolite blocks were also recovered in Luobusa and have ages of 86–80 Ma (Malpas et al., 2003). It is unclear at the moment whether these ages represent two discrete events or a prolonged emplacement event. The closeness between U–Pb zircon ages and ^{40}Ar – ^{39}Ar amphibole ages suggests the SSZ-type YZSZ oceanic lithosphere was young and hot when the metamorphic rocks were formed and some authors have recently suggested that the ages of metamorphic soles might be more closely related to ophiolite generation than emplacement (Dewey and Casey, 2011). The residual heat of the oceanic lithosphere could therefore have provided heat needed for metamorphism. The situation in southern Tibet is similar to the classical example of the Semail ophiolite, for which the time difference between crystallization and peak amphibolite metamorphism is less than 2 Ma (Hacker, 1994; Hacker and Gnos, 1997; Searle and Cox, 1999, 2002; Searle et al., 2004). The significance of the second group of amphibolites is uncertain, but it is possibly worth noting that the Spong arc in Ladakh has an age of 88 ± 5 Ma (Pedersen et al., 2001) and the Kohistan island arc in NW Pakistan has a similar age of 99–82 Ma (Schaltegger et al., 2002). A similar age of 80.2 ± 1.5 Ma has also been reported for the Muslim Bagh ophiolite (Kakar et al., 2012). These ages overlap with those for Late Cretaceous amphibolite blocks preserved in the mélanges in Xigaze and Luobusa areas (Malpas et al., 2003; Guilmette et al., 2009). This raises a possibility that the amphibolite blocks might have formed by a mechanism similar to that discussed above, but in a younger subduction zone, above which the island arc complex and its eastward extension formed. Whether the amphibolites in NW India are related to the Spong arc or Kohistan island arc remains an open question. Other evidence of such an Early Cretaceous SSZ event might have been destroyed during the India–Asia collision.

In southern central Tibet immediately south of the suture zone, the first appearance of ophiolitic detritus in sediments deposited on the margin of Greater India is recorded in the northern Tethyan Himalayan flysch succession in the late Paleocene (c. 57 Ma) (Ding et al., 2005; Aitchison et al., 2007a). A slightly younger Early Eocene age has been reported further to the south (Zhu et al., 2005) possibly indicating progression of a sedimentary wedge shedding southwards as the ophiolite was emplaced onto northern India. Moreover, the ophiolite tectonically overlies mélangé containing siliceous sediments with radiolarians as young as latest Paleocene (Liu and Aitchison, 2002; Liang et al., 2012). We note that, in Oman, ophiolitic detritus only appears in the foreland basin succession at the very top of the succession 20 million years after the obduction process is inferred to have begun and it is clear that stratigraphic data alone cannot be used to interpret timing of the entire emplacement event. In southern Tibet the whole SSZ package of ophiolite, turbidites and mélangé was eroded during the accumulation of syn-orogenic deposits such as the Paleocene–Lower Eocene Liuqu conglomerate (Davis et al., 2002). In Ladakh the Lamayuru thrust sheets that underlie the Spontang ophiolite are unconformably overlain by Late Maastrichtian (Marpo Fm.) and Paleocene–Early Eocene shallow marine limestones (Stumpata, Singie-la, Kesi formations; (Searle et al., 1997; Corfield et al., 1999; Green et al., 2008)). The ophiolite

is interpreted by some authors to have been emplaced onto the north Indian margin in the Late Cretaceous when obduction is postulated to have downflexed the passive margin and increased the sedimentation rate significantly (Searle et al., 1997; Corfield et al., 2005). Garzanti et al. (1987, 2005) suggested a later (post-Early Eocene) emplacement of the Spontang ophiolite based on the fact that along the southwestern margin the Spontang ophiolite has been thrust above Eocene shallow water limestones. Searle et al. (1988, 1997) showed that this was a later thrust that re-stacked the sequence and not the original obduction-related thrust. Corfield et al. (1999) sequentially restored all the structures in the Zaskar shelf and infer a two stage-thrusting event, the first of which they interpreted as pre-Paleocene obduction and the second as post-Eocene continental collision-related. Whatever the precise timing of their obduction, the ophiolites must have been emplaced prior to the final closing of Tethys Ocean.

7. Conclusion

A preponderance of dated SSZ ophiolitic rocks from along both the YTSZ and its lateral correlative the Indus Suture are of Early Cretaceous (Barremian to early Aptian; 130–120 Ma) age. Locally these rocks are associated with, and possibly built upon, MOR rocks of Late Jurassic age. Recently published hypotheses that link widespread rapid generation of ophiolites to forearc spreading during subduction initiation events (Dewey and Casey, 2011; Whattam and Stern, 2011) suggest this has important implications for understanding the evolution of the Tethyan Ocean and has important implications for regional geodynamic models.

Acknowledgements

Fieldwork was supported by HKU CRCG and the Research Grants Council of the Hong Kong Special Administrative Region, China (HKU 7001/04P) to Aitchison. U–Pb dating work was funded by NERC Isotope Geoscience laboratory grant 20427 to Searle. We thank N. Boulton and V. Pashely at NIGL for assistance in the operation of TIMS and MC-ICP-MS and C.-K. Lai and K.-S. Ma for whole-rock geochemistry sample preparation. Gavin Chan was funded by a Croucher Foundation Scholarship. We also thank two anonymous reviewers and the editors of this special issue for their assistance with our manuscript.

Appendix A. Supplementary data

Supplementary data associated with this article can be found in the online version, at <http://dx.doi.org/10.1016/j.gr.2013.06.016>. These data include Google maps of the most important areas described in this article.

References

- Abrajevitch, A., Ali, J.R., Aitchison, J.C., Badengzhu, Davis, A.M., Liu, J.B., Ziyabrev, S.V., 2005. Neotethys and the India–Asia collision: insights from a palaeomagnetic study of the Dazhuqu ophiolite southern Tibet. *Earth and Planetary Science Letters* 233, 87–102.
- Ahmed, Z., 1993. Leucocratic rocks from the Bela ophiolite, Khuzdar District, Pakistan. In: Treloar, P.J., Searle, M.P. (Eds.), *Himalayan Tectonics*. Geological Society, London, Special Publication, 74, pp. 89–100.
- Aitchison, J.C., Davis, A.M., 2004. Evidence for the multiphase nature of the India–Asia collision from the Yarlung Tsangpo suture zone, Tibet. In: Malpas, J.G., Fletcher, C.J.N., Ali, J.R., Aitchison, J.C. (Eds.), *Aspects of the Tectonic Evolution of China*. Geological Society of London, Special Publication, 226, pp. 217–233.
- Aitchison, J.C., Badengzhu, Davis, A.M., Liu, J., Luo, H., Malpas, J., McDermid, I., Wu, H., Ziyabrev, S., Zhou, M.F., 2000. Remnants of a Cretaceous intra-oceanic subduction system within the Yarlung–Zangbo suture (southern Tibet). *Earth and Planetary Science Letters* 183, 231–244.
- Aitchison, J.C., Abrajevitch, A., Ali, J.R., Badengzhu, Davis, A.M., Luo, H., Liu, J.B., McDermid, I.R.C., Ziyabrev, S., 2002a. New insights into the evolution of the Yarlung Tsangpo suture zone, Xizang (Tibet), China. *Episodes* 25, 90–94.
- Aitchison, J.C., Davis, A.M., Badengzhu, Luo, H., 2002b. New constraints on the India–Asia collision: the Lower Miocene Gangrinboche conglomerates, Yarlung Tsangpo suture zone, SE Tibet. *Journal of Asian Earth Sciences* 21, 253–265.
- Aitchison, J.C., Ali, J.R., Davis, A.M., 2007a. When and where did India and Asia collide? *Journal of Geophysical Research – Solid Earth* 112, B05423. <http://dx.doi.org/10.1029/2006JB004706>.
- Aitchison, J.C., McDermid, I.R.C., Ali, J.R., Davis, A.M., Ziyabrev, S.V., 2007b. Shoshonites in southern Tibet record Late Jurassic rifting of a Tethyan intra-oceanic island arc. *Journal of Geology* 115, 197–213.
- Aitchison, J.C., Ali, J.R., Chan, A., Davis, A.M., Lo, C.-H., 2009. Tectonic implications of felsic tuffs within the Lower Miocene Gangrinboche conglomerates, southern Tibet. *Journal of Asian Earth Sciences* 34, 287–297.
- Aitchison, J.C., Xia, X., Baxter, A.T., Ali, J.R., 2011. Detrital zircon U–Pb ages along the Yarlung–Tsangpo suture zone, Tibet: implications for oblique convergence and collision between India and Asia. *Gondwana Research* 20, 691–709.
- Ali, J.R., Aitchison, J.C., 2008. Gondwana to Asia: plate tectonics, paleogeography and the biological connectivity of the Indian sub-continent from the Middle Jurassic through latest Eocene (166–35 Ma). *Earth-Science Reviews* 88, 145–166.
- Allegre, C.J., Courtillot, V., Tapponnier, P., Hirt, A., Mattauer, M., Coulon, C., Jaeger, J.J., Achache, J., Schaerer, U., Marcoux, J., Burg, J.P., Girardeau, J., Armijo, R., Garipey, C., Goepel, C., Li, T.D., Xiao, X.C., Chang, C.F., Li, G.G., Lin, B.Y., Teng, J.W., Wang, N.W., Chen, G.M., Han, T.L., Wang, X.B., Den, W.M., Sheng, H.B., Cao, Y.G., Zhou, J., Qiu, H.R., Bao, P.S., Wang, S.C., Wang, B.X., Zhou, Y., Xu, R., 1984. Structure and evolution of the Himalaya–Tibet orogenic belt. *Nature* 307, 17–22.
- Bai, W., Zhou, M.F., Robinson, P.T., 1993. Possible diamond-bearing mantle peridotites and podiform chromitites in the Luobusa and Donqiao ophiolites, Tibet. *Canadian Journal of Earth Sciences = Journal Canadien des Sciences de la Terre* 30, 1650–1659.
- Bai, W., Robinson, P.T., Fang, Q., Yang, J., Yan, B., Zhang, Z., Hu, X.F., Zhou, M.F., Malpas, J., 2000. The PGE and base-metal alloys in the podiform chromitites of the Luobusa ophiolite, southern Tibet. *Canadian Mineralogist* 38, 585–598.
- Bao, P.S., Su, L., Wang, J., Zhai, Q.G., 2013. Study on the Tectonic Setting for the Ophiolites in Xigaze, Tibet. *Acta Geologica Sinica-English Edition* 87, 395–425.
- Baxter, A., Aitchison, J.C., Ali, J.R., Ziyabrev, S.V., 2010. Lower Cretaceous radiolarians from the Spontang massif, Ladakh, NW India: implications for Neo-Tethyan evolution. *Journal of the Geological Society of London* 167, 511–517.
- Bédard, E., Hébert, R., Guilmette, C., Lesage, G., Wang, C.S., Dostal, J., 2009. Petrology and geochemistry of the Saga and Sangsang ophiolitic massifs, Yarlung Zangbo Suture Zone, Southern Tibet: evidence for an arc-back-arc origin. *Lithos* 113, 48–67.
- Besse, J., Courtillot, V., 1988. Paleogeographic maps of the continents bordering the Indian ocean since the Early Jurassic. *Journal of Geophysical Research* 93, 11791–11808.
- Burg, J.P., 2011. The Asia–Kohistan–India Collision: Review and Discussion. In: Brown, D., Ryan, P.D. (Eds.), *Arc–Continent Collision*. Springer, Berlin Heidelberg, pp. 279–309.
- Chan, H.N., 2008. Petrogenesis and tectonic evolution of Yarlung Tsangpo ophiolites, south Tibet. (D. Phil thesis) Department of Earth Sciences, University of Oxford (152 pp.).
- Coffin, M.F., Rabinowitz, P.D., 1987. Reconstruction of Madagascar and Africa: evidence from the Davie Fracture Zone and Western Somali Basin. *Journal of Geophysical Research* 92, 9385–9406.
- Corfield, R.I., Searle, M.P., Green, O.R., 1999. Photang thrust sheet; an accretionary complex structurally below the Spontang Ophiolite constraining timing and tectonic environment of ophiolite obduction, Ladakh Himalaya, NW India. *Journal of the Geological Society of London* 156, 1031–1044.
- Corfield, R.I., Searle, M.P., Pedersen, R.B., 2001. Tectonic Setting, Origin, and Obduction History of the Spontang Ophiolite, Ladakh Himalaya, NW India. *Journal of Geology* 109, 715–736.
- Corfield, R.I., Watts, A.B., Searle, M.P., 2005. Subsidence history of the north Indian continental margin, Zaskar–Ladakh Himalaya, NW India. *Journal of the Geological Society of London* 162, 135–146.
- Dai, J.-G., Wang, C.-S., Hébert, R., Santosh, M., Li, Y.-L., Xu, J.-Y., 2011. Petrology and geochemistry of peridotites in the Zhongba ophiolite, Yarlung Zangbo Suture Zone: implications for the Early Cretaceous intra-oceanic subduction zone within the Neo-Tethys. *Chemical Geology* 288, 133–148.
- Dai, J., Wang, C., Polat, A., Santosh, M., Li, Y., Ge, Y., 2013. Rapid forearc spreading between 130–120 Ma: evidence from geochronology and geochemistry of the Xigaze ophiolite, southern Tibet. *Lithos* 172–173, 1–16.
- Davis, A.M., Aitchison, J.C., Badengzhu, Luo, H., Ziyabrev, S., 2002. Paleogene island arc collision-related conglomerates, Yarlung–Tsangpo suture zone, Tibet. *Sedimentary Geology* 150, 247–273.
- Dewey, J.F., Casey, J.F., 2011. The Origin of Obducted Large-Slab Ophiolite Complexes. In: Brown, D., Ryan, P.D. (Eds.), *Arc–Continent Collision*. Springer, Berlin Heidelberg, pp. 431–444.
- Ding, L., Kapp, P., Wan, X., 2005. Paleocene–Eocene record of ophiolite obduction and initial India–Asia collision, south central Tibet. *Tectonics* 24, TC3001. <http://dx.doi.org/10.1029/2004TC001729>.
- Dubois-Cote, V., Hébert, R., Dupuis, C., Wang, C.S., Li, Y.L., Dostal, J., 2005. Petrological and geochemical evidence for the origin of the Yarlung Zangbo ophiolites, southern Tibet. *Chemical Geology* 214, 265–286.
- Dürr, S.B., 1996. Provenance of Xigaze fore-arc basin clastic rocks (Cretaceous, South Tibet). *Geological Society of America Bulletin* 108, 669–684.
- Gansser, A., 1964. *The Geology of the Himalayas*. Wiley-Interscience, New York (289 pp.).
- Garzanti, E., Baud, A., Mascle, G., 1987. Sedimentary record of the northward flight of India and its collision with Eurasia (Ladakh Himalaya, India). *Geodinamica Acta* 1, 297–312.
- Garzanti, E., Sciuonach, D., Gaetani, M., Corfield, R.I., Searle, M.P., Watts, A.B., 2005. Discussion on subsidence history of the north Indian continental margin, Zaskar–Ladakh Himalaya, NW India. *Journal of the Geological Society of London* 162, 889–892.

- Ghazi, A.M., Hassanipak, A.A., Mahoney, J.J., Duncan, R.A., 2004. Geochemical characteristics, ^{40}Ar – ^{39}Ar ages and original tectonic setting of the Band-e-Zeyar/Dar Anar ophiolite, Makran accretionary prism, S.E. Iran. *Tectonophysics* 393, 175–196.
- Gibbons, A.D., Barckhausen, U., van den Bogaard, P., Hoernle, K., Werner, R., Whittaker, J.M., Müller, R.D., 2012. Constraining the Jurassic extent of Greater India: tectonic evolution of the West Australian margin. *Geochemistry, Geophysics, Geosystems* 13, Q05W13.
- Girardeau, J., Mercier, J.C., Xibin, W., 1985a. Petrology of the mafic rocks of the Xigaze ophiolite, Tibet: implications for the genesis of the oceanic lithosphere. *Contributions to Mineralogy and Petrology* 90, 309–321.
- Girardeau, J., Mercier, J.C.C., Zao, Y.G., 1985b. Origin of the Xigaze Ophiolite, Yarlung Zangbo suture zone, southern Tibet. *Tectonophysics* 119, 407–433.
- Girardeau, J., Mercier, J.C.C., Zao, Y.G., 1985c. Structure of the Xigaze Ophiolite, Yarlung Zangbo suture zone, southern Tibet, China; genetic implications. *Tectonics* 4, 267–288.
- Goodenough, K., Styles, M., Schofield, D., Thomas, R., Crowley, Q., Lilly, R., McKervey, J., Stephenson, D., Carney, J., 2010. Architecture of the Oman–UAE Ophiolite: evidence for a multi-phase magmatic history. *Arabian Journal of Geosciences* 3, 439–458.
- Göpel, C., Allegre, C.J., Rong, H.X., 1984. Lead isotopic study of the Xigaze ophiolite (Tibet); the problem of the relationship between magmatites (gabbros, dolerites, lavas) and tectonites (harzburgites). *Earth and Planetary Science Letters* 69, 301–310.
- Gradstein, F.M., Ogg, J.G., Schmitz, M., Ogg, G., 2012. *The Geologic Time Scale 2012*. Elsevier (2-Volume Set).
- Green, O.R., Searle, M.P., Corfield, R.I., Corfield, R.M., 2008. Cretaceous–Tertiary Carbonate Platform Evolution and the Age of the India–Asia Collision along the Ladakh Himalaya (Northwest India). *Journal of Geology* 116, 331–353.
- Griselin, M., Davies, G.R., Pearson, D.G., 1999. REE and Sr–Pb–Nd isotope geochemistry of Tibetan peridotites: implications for melting processes. *Ophiolite* 24, 102–103.
- Guilmette, C., Hébert, R., Dupuis, C., Wang, C., Li, Z., 2007. Metamorphic history and geodynamic significance of high-grade metabasites from the ophiolitic mélange beneath the Yarlung Zangbo ophiolites, Xigaze area, Tibet. *Journal of Asian Earth Sciences*. <http://dx.doi.org/10.1016/j.jseas.2007.10.111>.
- Guilmette, C., Hébert, R., Wang, C., Villeneuve, M., 2009. Geochemistry and geochronology of the metamorphic sole underlying the Xigaze Ophiolite, Yarlung Zangbo Suture Zone, South Tibet. *Lithos* 112, 149–162.
- Guilmette, C., Hébert, R., Dostal, J., Indares, A., Ullrich, T., Bédard, É., Wang, C., 2012. Discovery of a dismembered metamorphic sole in the Saga ophiolitic mélange, South Tibet: assessing an Early Cretaceous disruption of the Neo-Tethyan supra-subduction zone and consequences on basin closing. *Gondwana Research* 22, 398–414.
- Guo, T.Y., Liang, D.Y., Zhang, Y.Z., Zhao, C.H., 1991. *Geology of Ngari Tibet (Xizang)*. Chinese University of Geosciences Press, Beijing (464 pp.).
- Hacker, B.R., 1994. Rapid emplacement of young oceanic lithosphere: argon geochronology of the Oman ophiolite. *Science* 265, 1563–1565.
- Hacker, B.R., Gnos, E., 1997. The conundrum of Samail: explaining the metamorphic history. *Tectonophysics* 279, 215–226.
- Hébert, R., Huot, F., Wang, C., Liu, Z., 2003. Yarlung Zangbo ophiolites (Southern Tibet) revisited: geodynamic implications from the mineral record. In: Dilek, Y., Robinson, P.T. (Eds.), *Geological Society, London, Special Publications*, 218, pp. 165–190.
- Hébert, R., Bezard, R., Guilmette, C., Dostal, J., Wang, C.S., Liu, Z.F., 2012. The Indus–Yarlung Zangbo ophiolites from Nanga Parbat to Namche Barwa syntaxes, southern Tibet: first synthesis of petrology, geochemistry, and geochronology with incidences on geodynamic reconstructions of Neo-Tethys. *Gondwana Research* 22, 377–397.
- Horstwood, M.S.A., Foster, G.L., Parrish, R.R., Noble, S.R., Nowell, G.M., 2003. Common-Pb corrected in situ U–Pb accessory mineral geochronology by LA-MC-ICP-MS. *Journal of Analytical Atomic Spectrometry* 18, 837–846.
- Jenner, G., Dunning, G., Malpas, J., Brown, M., Brace, T., 1991. Bay of Islands and Little Port complexes, revisited: age, geochemical and isotopic evidence confirm suprasubduction-zone origin. *Canadian Journal of Earth Sciences* 28, 1635–1652.
- Ji, W.-Q., Wu, F.-Y., Chung, S.-L., Li, J.-X., Liu, C.-Z., 2009. Zircon U–Pb geochronology and Hf isotopic constraints on petrogenesis of the Gangdese batholith, southern Tibet. *Chemical Geology* 262, 229–245.
- Ji, W.-Q., Wu, F.-Y., Liu, C.-Z., Chung, S.-L., 2012. Early Eocene crustal thickening in southern Tibet: new age and geochemical constraints from the Gangdese batholith. *Journal of Asian Earth Sciences* 53, 82–95.
- Kakar, M.I., Collins, A.S., Mahmood, K., Foden, J.D., Khan, M., 2012. U–Pb zircon crystallization age of the Muslim Bagh ophiolite: enigmatic remains of an extensive pre-Himalayan arc. *Geology* 40, 1099–1102.
- Khan, M., Kerr, A.C., Mahmood, K., 2007. Formation and tectonic evolution of the Cretaceous–Jurassic Muslim Bagh ophiolitic complex, Pakistan: implications for the composite tectonic setting of ophiolites. *Journal of Asian Earth Sciences* 31, 112–127.
- Lee, H.-Y., Chung, S.-L., Lo, C.-H., Ji, J., Lee, T.-Y., Qian, Q., Zhang, Q., 2009. Eocene Neotethyan slab breakoff in southern Tibet inferred from the Linzizong volcanic record. *Tectonophysics* 477, 20–35.
- Li, J., Xia, B., Liu, L., Xu, L., He, G., Wang, H., Zhang, Y., Yang, Z., 2008. SHRIMP U–Pb dating of dolerite in the La'nga Co ophiolite, Burang, Tibet, China, and its geological significance. *Geological Bulletin of China* 27, 1739–1743.
- Li, J., Xia, B., Liu, L., Xu, L., He, G., Wang, H., Zhang, Y., Yang, Z., 2009. SHRIMP U–Pb dating for the Gabbro in Qunrang Ophiolite, Tibet: the geochronology constraint for the development of eastern Tetyas basin. *Geotectonica et Metallogenia* 33, 294–298.
- Liang, Y., Zhang, K., Xu, Y., He, W., An, X., Yang, Y., Jin, J., 2012. Late Paleocene radiolarian fauna from Tibet and its geological implications. *Canadian Journal of Earth Sciences* 49, 1–8.
- Liu, J.B., Aitchison, J.C., 2002. Upper Paleocene radiolarians from the Yamdrok mélange, south Xizang (Tibet), China. *Micropaleontology* 48, 145–154.
- Liu, C.-Z., Wu, F.-Y., Wilde, S.A., Yu, L.-J., Li, J.-L., 2010. Anorthitic plagioclase and pargasitic amphibole in mantle peridotites from the Yungbwa ophiolite (southwestern Tibetan Plateau) formed by hydrous melt metasomatism. *Lithos* 114, 413–422.
- Ludwig, K.R., 2003. *Isoplot 3.00. A Geochronological Toolkit for Microsoft Excel*, vol. 4. Berkeley Geochronology Center, Berkeley, California (70 pp.).
- Mahéo, G., Bertrand, H., Guillot, S., Villa, I.M., Keller, F., Capiez, P., 2004. The South Ladakh ophiolites (NW Himalaya, India): an intra-oceanic tholeiitic arc origin with implication for the closure of the Neo-Tethys. *Chemical Geology* 203, 273–303.
- Mahmood, K., Boudier, F., Gnos, E., Monié, P., Nicolas, A., 1995. $^{40}\text{Ar}/^{39}\text{Ar}$ dating of the emplacement of the Muslim Bagh ophiolite, Pakistan. *Tectonophysics* 254, 169–181.
- Malpas, J., 1979. The dynamothermal aureole of the Bay of Islands ophiolite suite. *Canadian Journal of Earth Sciences* 16, 2086–2101.
- Malpas, J., Zhou, M.-F., Robinson, P.T., Reynolds, P.H., 2003. Geochemical and geochronological constraints on the origin and emplacement of the Yarlung Zangbo ophiolites, Southern Tibet. *Geological Society, London, Special Publications* 218, 191–206.
- Mattinson, J.M., 2005. Zircon U–Pb chemical abrasion (“CA-TIMS”) method: combined annealing and multi-step partial dissolution analysis for improved precision and accuracy of zircon ages. *Chemical Geology* 220, 47–66.
- McDermid, I.R.C., Aitchison, J.C., Davis, A.M., Harrison, T.M., Grove, M., 2002. The Zedong terrane: a Late Jurassic intra-oceanic magmatic arc within the Yarlung–Zangbo suture zone, southeastern Tibet. *Chemical Geology* 187, 267–277.
- Metcalfe, R.V., Wallin, E.T., Willse, K.R., Muller, E.R., 2000. *Geology and geochemistry of the ophiolitic Trinity terrane, California: evidence of middle Paleozoic depleted supra-subduction zone magmatism in a proto-arc setting*. In: Dilek, Y., Moores, E.M., Elthon, D., Nicolas, A. (Eds.), *Ophiolites and oceanic crust: new insights from field studies and the Ocean Drilling Program*. Geological Society of America Special Paper, 349, pp. 403–418.
- Miller, C., Thöni, M., Frank, W., Schuster, R., Melcher, F., Meisel, T., Zanetti, A., 2003. Geochemistry and tectonomagmatic affinity of the Yungbwa ophiolite, SW Tibet. *Lithos* 66, 155–172.
- Mundil, R., Ludwig, K.R., Metcalfe, I., Renne, P.R., 2004. Age and timing of the Permian mass extinctions: U/Pb dating of closed-system zircons. *Science* 305, 1760–1763.
- Nicolas, A., Girardeau, J., Marcoux, J., Dupre, B., Wan, X., Cao, Y., Zheng, H., Xiao, X., 1981. The Xigaze ophiolite (Tibet): a peculiar oceanic lithosphere. *Nature* 294, 414–417.
- Noble, S., Schwieters, J., Condon, D., Crowley, Q., Quaas, N., Parrish, R., 2006. TIMS characterization of new generation secondary electron multiplier. *AGU 2006 Fall Meeting Abstracts (V11E-06)*.
- Pedersen, R.B., Searle, M.P., Corfield, R.I., 2001. U–Pb zircon ages from the Spontang Ophiolite, Ladakh Himalaya. *Journal of the Geological Society of London* 158, 513–520.
- Robinson, P.T., Bai, W.-J., Malpas, J., Yang, J.-S., Zhou, M.-F., Fang, Q.-S., Hu, X.-F., Cameron, S., Staudigel, H., 2004. Ultra-high pressure minerals in the Luobusa Ophiolite, Tibet, and their tectonic implications. *Geological Society, London, Special Publications* 226, 247–271.
- Schaltegger, U., Zellinger, G., Frank, M., Burg, J.-P., 2002. Multiple mantle sources during island arc magmatism: U–Pb and Hf isotopic evidence from the Kohistan arc complex, Pakistan. *Terra Nova* 14, 461–468.
- Searle, M.P., 1983. Stratigraphy, structure and evolution of the Tibetan–Tethys zone in Zanskar and the Indus suture zone in the Ladakh Himalaya. *Transactions of the Royal Society of Edinburgh: Earth Sciences* 73, 205–219.
- Searle, M.P., 1986. Structural evolution and sequence of thrusting in the High Himalayan, Tibetan–Tethys and Indus suture zones of Zanskar and Ladakh, western Himalaya. *Journal of Structural Geology* 8, 923–936.
- Searle, M., Cox, J., 1999. Tectonic setting, origin, and obduction of the Oman ophiolite. *Geological Society of America Bulletin* 111, 104–122.
- Searle, M.P., Cox, J., 2002. Subduction zone metamorphism during formation and emplacement of the Semail ophiolite in the Oman Mountains. *Geological Magazine* 139, 241–255.
- Searle, M., Malpas, J., 1982. Petrochemistry and origin of sub-ophiolitic metamorphic and related rocks in the Oman Mountains. *Journal of the Geological Society of London* 139, 235–248.
- Searle, M.P., Treloar, P.J., 2010. Was Late Cretaceous–Paleocene obduction of ophiolite complexes the primary cause of crustal thickening and regional metamorphism in the Pakistan Himalaya? In: Kusky, T.M., Zhai, M.-G., Xiao, W. (Eds.), *The Evolving Continents: Understanding Processes of Continental Growth*. Geological Society, London, Special Publication, 338, pp. 345–359.
- Searle, M.P., Cooper, D.W.J., Rex, A.J., 1988. Collision tectonics of the Ladakh–Zanskar Himalaya. *Philosophical Transactions of the Royal Society of London. Series A: Mathematical and Physical Sciences* 326, 117–150.
- Searle, M.P., Corfield, R.I., Stephenson, B., McCarron, J., 1997. Structure of the North Indian continental margin in the Ladakh–Zanskar Himalayas: implications for the timing of obduction of the Spontang ophiolite, India–Asia collision and deformation events in the Himalaya. *Geological Magazine* 134, 297–316.
- Searle, M.P., Warren, C.J., Waters, D.J., Parrish, R.R., 2004. Structural evolution, metamorphism and restoration of the Arabian continental margin, Saih Hatat region, Oman Mountains. *Journal of Structural Geology* 26, 451–473.
- Simonetti, A., Heaman, L.M., Hartlaub, R.P., Creaser, R.A., MacHattie, T.G., Böhm, C., 2005. U–Pb zircon dating by laser ablation–MC–ICP–MS using a new multiple ion counting Faraday collector array. *Journal of Analytical Atomic Spectrometry* 20, 677–686.
- Stacey, J.S., Kramers, J., 1975. Approximation of terrestrial lead isotope evolution by a two-stage model. *Earth and Planetary Science Letters* 26, 207–221.
- Stampfli, G.M., Borel, G.D., 2002. A plate tectonic model for the Paleozoic and Mesozoic constrained by dynamic plate boundaries and restored synthetic oceanic isochrons. *Earth and Planetary Science Letters* 196, 17–33.
- Styles, M., Ellison, R., Arkley, S., Crowley, Q., Farrant, A., Goodenough, K., McKervey, J., Pharaoh, T., Phillips, E., Schofield, D., 2006. *The geology and geophysics of the United Arab Emirates*. Geology (Ministry of Energy, Petroleum and Minerals, Abu Dhabi, United Arab Emirates).
- Wakabayashi, J., Dilek, Y., 2000. Spatial and temporal relationships between ophiolites and their metamorphic soles: a test of models of forearc ophiolite genesis. In: Dilek,

- Y., Moores, E.M., Elthon, D., Nicholas, A. (Eds.), *Ophiolites and oceanic crust: new insights from field studies and the Ocean Drilling Program*. Geological Society of America Special Paper, 349, pp. 53–64.
- Wang, X.B., Bao, P.S., Xiao, X.C., 1987. *Ophiolites of the Yarlung Zangbo (Tsangbo) River, Xizang (Tibet)*. Publishing House of Surveying and Mapping (118 pp. plus foldout Geological Map of the Ophiolite Zone along the Middle Yarlung Zangbo (Tsangbo) River, Xizang (Tibet), Beijing).
- Wang, R., Xia, B., Zhou, G.Q., Zhang, Y.Q., Yang, Z.Q., Li, W.Q., Wei, D.L., Zhong, L.F., Xu, L.F., 2006. SHRIMP zircon U–Pb dating for gabbro from the Tiding ophiolite in Tibet. *Chinese Science Bulletin* 51, 1776–1779.
- Wang, C., Li, X., Liu, Z., Li, Y., Jansa, L., Dai, J., Wei, Y., 2012. Revision of the Cretaceous–Paleogene stratigraphic framework, facies architecture and provenance of the Xigaze forearc basin along the Yarlung Zangbo suture zone. *Gondwana Research* 22, 415–433.
- Warren, C.J., Parrish, R.R., Searle, M.P., Waters, D.J., 2003. Dating the subduction of the Arabian continental margin beneath the Semail ophiolite, Oman. *Geology* 31, 889–892.
- Wei, D.L., Xia, B., Zhang, Y.Q., Wang, R., Yang, Z.Q., Wei, D.L., 2006. SHRIMP zircon dating of diabase in the Xiugugabu ophiolite in Tibet and its geological implications. *Geotectonica et Metallogenia* 27, 31–34.
- Whattam, S., Stern, R., 2011. The 'subduction initiation rule': a key for linking ophiolites, intra-oceanic forearcs, and subduction initiation. *Contributions to Mineralogy and Petrology* 162, 1031–1045.
- Williams, H.R., Smythe, W.R., 1973. Metamorphic aureoles beneath ophiolite suites and Alpine peridotites. Tectonic implications with west Newfoundland examples. *American Journal of Science* 273, 594–621.
- Xia, B., Jianfeng, L., Xu, L., Wang, R., Yang, Z., 2011. Sensitive high resolution ion microprobe U–Pb zircon geochronology and geochemistry of mafic rocks from the Pulan-Xiangquanhe Ophiolite, Tibet: constraints on the evolution of the neo-Tethys. *Acta Geologica Sinica-English Edition* 85, 840–853.
- Xiong, F.H., Yang, J.S., Liang, F.H., Ba, D.Z., Zhang, J., Xu, X.Z., Li, Y., Liu, Z., 2011. Zircon U–Pb ages of the Dongbo ophiolite, in the western Yariung Zangbo suture zone and their geological significance. *Acta Petrologica Sinica* 27, 3223–3238.
- Yamamoto, H., Yamamoto, S., Kaneko, Y., Terabayashi, M., Komiya, T., Katayama, I., Iizuka, T., 2007. Imbricate structure of the Luobusa Ophiolite and surrounding rock units, southern Tibet. *Journal of Asian Earth Sciences* 29, 296–304.
- Zhong, L.F., Xia, B., Zhang, Y.Q., Wang, R., Wei, D.L., Yang, Z.Q., 2006a. Origin of the Luobusa ophiolite, southern Tibet: Sr–Nd–Pb isotopic constraints on crust lavas. *Journal of Mineralogy and Petrology* 26, 57–63.
- Zhong, L.F., Xia, B., Zhang, Y.Q., Wang, R.L., Wei, D.L., Yang, Z.Q., 2006b. SHRIMP Age Determination of the Diabase in Luobusa Ophiolite, Southern Xizang (Tibet). *Geological Review* 52, 224–229.
- Zhou, M.F., Robinson, P.T., Malpas, J., Li, Z., 1996. Podiform chromitites in the Luobusa Ophiolite (southern Tibet): implications for melt–rock interaction and chromite segregation in the upper mantle. *Journal of Petrology* 37, 3–21.
- Zhou, S., Mo, X.X., Mahoney, J.J., Zhang, S.Q., Guo, T.J., Zhao, Z.D., 2002. Geochronology and Nd and Pb isotope characteristics of gabbro dikes in the Luobusa ophiolite, Tibet. *Chinese Science Bulletin* 47, 143–146.
- Zhou, M.-F., Robinson, P.T., Malpas, J., Edwards, S.J., Qi, L., 2005. REE and PGE geochemical constraints on the formation of dunites in the Luobusa Ophiolite, southern Tibet. *Journal of Petrology* 46, 615–639.
- Zhu, B., Kidd, W.S.F., Rowley, D.B., Currie, B.S., Shafique, N., 2005. Age of initiation of the India–Asia collision in the East-Central Himalaya. *Journal of Geology* 113, 265–285.
- Ziabrev, S.V., Aitchison, J.C., Abrajevitch, A., Badengzhu, Davis, A.M., Luo, H., 2003. Precise radiolarian age constraints on the timing of ophiolite generation and sedimentation in the Dazhuqu terrane, Yarlung-Tsangpo suture zone, Tibet. *Journal of the Geological Society of London* 160, 591–600.
- Zyabrev, S.V., Kojima, S., Ahmad, T., 2008. Radiolarian biostratigraphic constraints on the generation of the Nidar ophiolite and the onset of Dras arc volcanism: tracing the evolution of the closing Tethys along the Indus–Yarlung-Tsangpo suture. *Stratigraphy* 5, 99–112.